CHALMERS

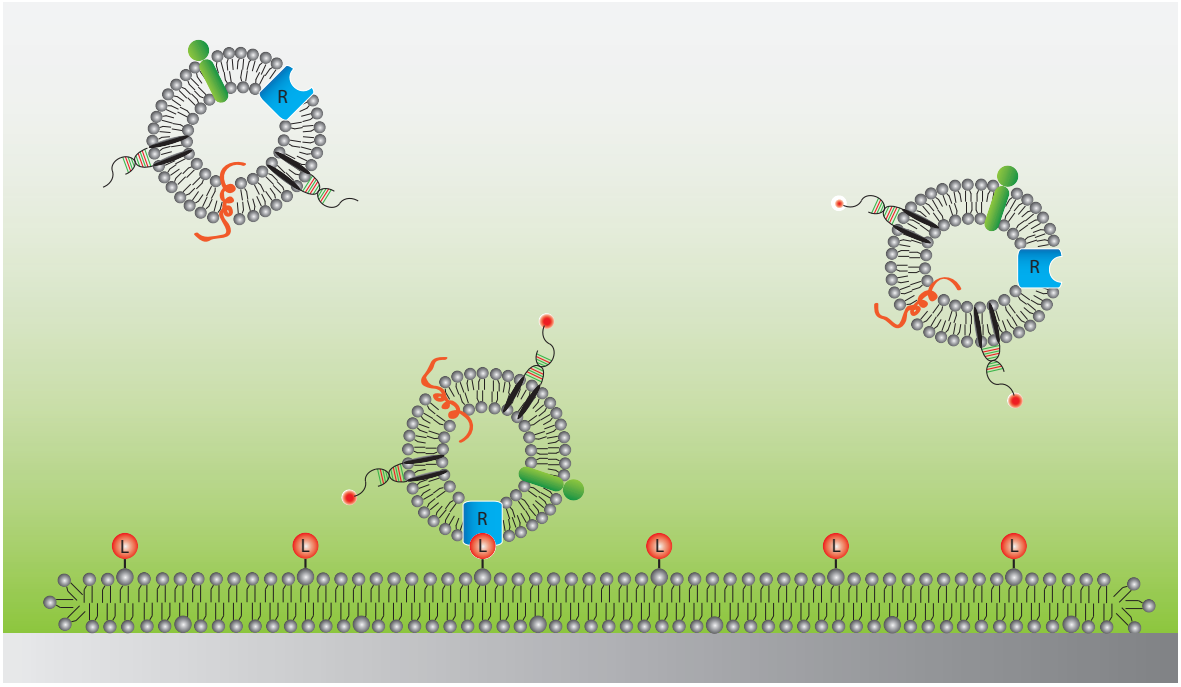

Characterizing the kinetics of human ligand-receptor interactions with single molecule sensitivity

Master's Thesis in Applied Physics

OLOV WAHLSTEN

Department of Applied Physics
Division of Biological Physics
Chalmers University of Technology
Göteborg, Sweden 2012

THESIS FOR THE DEGREE OF MASTER OF SCIENCE

Characterizing the kinetics of human ligand-receptor interactions with single molecule sensitivity

OLOV WAHLSTEN

CHALMERS

Department of Applied Physics
Division of Biological Physics
Chalmers University of Technology
Göteborg, Sweden 2012

Characterizing the kinetics of human ligand-receptor interactions with single molecule sensitivity

OLOV WAHLSTEN

Department of Applied Physics
Division of Biological Physics
SE-412 96 Göteborg
Sweden
Telephone +46(0)31-772 10 00

Printed at Chalmers Reproservice Göteborg, 2012

Cover illustration: *Fluorescent molecules incorporated into the membrane of vesicles, derived from a cell membrane, containing the G-protein coupled receptor (R) excited by an evanescent field originating from total internal reflection enable characterization of the interaction between this receptor and one of its chemokine ligands (L) with a single molecule sensitivity.*

Characterizing the kinetics of human ligand-receptor interactions with single molecule sensitivity

OLOV WAHLSTEN

Department of Applied Physics
Division of Biological Physics
Chalmers University of Technology
Göteborg, Sweden 2012

Abstract

Membrane proteins represent about two thirds of the protein targets for existing drugs. Therefore, studies of this class of proteins is a very important part of the drug discovery process. Large drug developing companies put enormous resources on getting new products into the market, motivating new and more efficient means for the characterization of potential drugs.

In this thesis a method with single molecule sensitivity is investigated for the characterization of the interaction between a G-Protein Coupled Receptor (GPCR) and one of its natural ligands. GPCRs are estimated to be targeted by more than 40% of the drugs used in clinical medicine, making them the pharmaceutically most important subclass of membrane proteins. In this project the CXCR3 receptor is studied along with its chemokine ligand CXCL10. This receptor-ligand couple plays an important role in our immune system and diseases such as multiple sclerosis and type 1 diabetes are related to the CXCR3 receptor. The approach is to immobilize ligands on a surface and use fluorescently labeled vesicles, derived from membranes of cells expressing the CXCR3 transmembrane protein, in order to visualize the ligand-receptor interaction. The initial evaluation of the surface chemistry was performed with the Quartz Crystal Microbalance with Dissipation monitoring (QCMD) technique. Bind and release events between receptor and ligand were monitored under equilibrium with single event resolution using Total Internal Reflection Fluorescence Microscopy (TIRFM). Kinetic parameters characterizing the interaction were extracted from statistics on these bind and release events.

k_{off} and k_{on} for the interaction between the CXCR3 receptor and the CXCL10 ligand were determined to $6.7 \cdot 10^{-4}\, s^{-1}$ and $4.0 \cdot 10^{4}\, s^{-1}M^{-1}$, respectively. The equilibrium dissociation constant, K_d, was determined implicitly to $16.8\, nM$ and theoretically to $0.3\, nM$.

Keywords: Drug discovery, GPCR, pharmacodynamics, equilibrium fluctuation analysis, kinetics, TIRFM, QCMD.

Acknowledgements

I would like to take the opportunity to acknowledge the people contributing to this thesis in one or the other way. I have learned a lot during this spring and the master's thesis project had never been practicable for me without you. The individual order in which people are notified does not mean anything particular, it only demonstrates the known fact that you tend to get more emotional at the end of writing an acknowledgement.

Biological Physics group, where I have done my master's thesis project. I really appreciate the atmosphere and the open arm welcoming of a new master student.

Main supervisor *Fredrik Höök*. All enlightening discussions and inspiring ideas have been invaluable in this project. Co-supervisors *Anders Gunnarsson* and *Lisa Simonsson*, for all the great ideas and for introducing me to the laboratory environment. To all of you: your great knowledge, support, sunny mood and patience have definitely made this spring to one of the better.

Peter Apell, for introducing me to the area of biological physics and in this project being involved in the theoretical work. We have collaborated in many projects recent years and I really appreciate you for giving me the opportunity.

Friends at Engineering Physics who made the whole education to a much more pleasant experience. The number of lunch boxes and laughs we have shared must be on the list of "top ten integers closest to infinity".

Family members and *relatives*. Your guidance and support in combination with the non-entropic behaviour of myself has led me through the bifurcation pattern of the more and less fateful decisions in life.

Cecilia, for all support, interest, belief and for being jealous of my project. I love you.

Olov Wahlsten, Göteborg, 4 June 2012

Contents

1 Introduction **1**
- 1.1 Background and motivation . . . 1
- 1.2 Outline . . . 2

2 Biological foundation **4**
- 2.1 Life and its fundamental building blocks . . . 4
- 2.2 The cell membrane . . . 5
- 2.3 Mimicing a simplified nature . . . 6

3 Pharmacodynamics **7**
- 3.1 Ligand-receptor interaction . . . 7
- 3.2 The Langmuir model . . . 8
- 3.3 Inhibition by an antagonist . . . 11

4 Methodology **12**
- 4.1 Quartz Crystal Microbalance with Dissipation monitoring - QCMD . . . 13
  - 4.1.1 Bilayer formation in QCMD . . . 14
- 4.2 Total Internal Reflection Fluorescence Microscopy - TIRFM . . . 15
  - 4.2.1 Bilayer formation in TIRFM . . . 17

5 Immobilizing ligands on a surface **18**
- 5.1 CXCL10 immobilized on POPC-bilayer . . . 19

6 Fluorescent labeling of cell mimics **21**
- 6.1 Vybrant DiI and FM1-43 . . . 22
- 6.2 ds-2TAM/3 . . . 23

7 Equilibrium fluctuation analysis **25**
- 7.1 Image analysis . . . 26
- 7.2 Determination of kinetic parameters . . . 27

8 Theoretical aspects **29**
- 8.1 Theoretical equilibrium dissociation constant . . . 29
- 8.2 Changes in enthalpy and entropy . . . 32

8.3 Influence of flow 33

9 Conclusions **36**
9.1 Immobilizing ligands on a surface 36
9.2 Fluorescent labeling of cell mimics 37
9.3 Equilibrium fluctuation analysis 37
9.4 Theoretical aspects 37

10 Future perspectives **38**

Bibliography **41**

A List of abbreviations **42**

"Equipped with his five senses, man explores the universe around him and calls the adventure Science."

Edwin Hubble

1

Introduction

The nature surrounding us is an inexhaustible source of ingenious solutions to a multitude of challenges. The human species has studied it for thousands of years in purpose of simplifying its own living conditions, but also in curiosity. For example we learned the existence of fire from lightning striking the ground and imitated birds in order to enable human flight.

In the early stage of human life our mind was restricted to a frame that was either directly observable or indirectly reachable. From the smallest grain of sand to the most vast plains and fields. As time passed on we gained more and more knowledge about our place in the universe and different optical appliances facilitated growth of this frame of awareness. Today this frame spans more than 40 orders of magnitude. From the atomic nucleus to the estimated diameter of the observable universe [1, 2].

Also, we have learned that complex systems exist at all these length scales. However, it is evident that many similar structures exist at different length scales. This is termed self-similarity and is the basis for fractal patterns. Striking examples are that the smallest leafs of the fern looks like the largest ones and that a branch of a tree is like a small tree itself. Fractal patterns are often very complex but are generated with simple rules that are repeated. A little bit of randomness in each step makes every macroscopic object totally unique. In our world there are enormous scientific fields to study, but is the complexity of ingoing systems always so intricate, or is it sometimes just simple rules repeated? However, one thing that is for sure is that we constantly learn more about these complex systems.

1.1 Background and motivation

There is an endless number of naturally occurring processes that we humans have not fully understood. The closest example may be our own bodies, where billions and billions of molecules interact every second. One very important and also very complex system within the body is the immune system. Its function is to detect and incapacitate foreign and harmful

substances in the body. Without the immune system we would likely face death in a relatively near future. Medicine and pharmaceutics also play an important role in recovering from disease and for us to stay healthy. Specialized proteins with communicative functions residing in the cell membrane, so called membrane receptors, are pharmaceutically important since many drugs target them to trigger changes in the function of the cell. The formation of a complex between the receptor and another molecule, so called ligand, is what triggers the response.

The aim of this project has been to investigate a high-sensitivity method for characterizing ligand-receptor interactions occurring in a near natural environment. Conventional methods, such as the Biacore^{TM} based on Surface Plasmon Resonance (SPR), are challenged by the low expression-level of membrane proteins in native cells and have trouble with preserving the natural environment for the proteins [3]. The high sensitivity of the method used in this project makes it potentially possible to study membrane proteins without over-expressing them. Furthermore, the method allows the membrane proteins to stay in a near native environment preserving their natural function. Single binding events are possible to detect, and kinetic parameters classifying the interaction could be extracted from statistics on these events at equilibrium.

The G-protein coupled receptor (GPCR) CXCR3, which is a transmembrane protein, along with one of its human chemokine ligands, CXCL10, have been studied. The GPCRs detect extracellular ligands and transduce signals into the cell. Diseases such as depression, schizophrenia and Parkinson's disease are related to these receptors [4]. GPCRs are estimated to be targeted by more than 40% of the drugs used in clinical medicine, making them the pharmaceutically most important subclass of membrane proteins [5]. The CXCR3 receptor is expressed on so called T helper cells, that play a key role in our immune system. The binding of CXCL10 to the CXCR3 induces a conformational change of the T helper cell making it migrate towards the site of inflammation [6]. The intention is that the project will lead to an increased knowledge on high-sensitivity drug screening methods as an alternative to conventional screening methods, where the membrane proteins must be over-expressed and thus not kept in a natural environment.

1.2 Outline

An introduction to biological physics and a description of the basic approaches utilized in the project will first be given. These parts may be most relevant for the ones not already in the field. Then, different methods and experiments leading to the goal of the project are enlightened. The outline of the report is further itemized below.

- **Chapter 2 - Biological foundation:** The chapter gives a short overview of life and its fundamental building blocks. The cell membrane and why mimics of it is so important in biological physics is also treated.
- **Chapter 3 - Pharmacodynamics:** The chapter briefly covers the theory on drug molecule kinetics but also regular ligand-receptor interaction. The reader will now have the basic knowledge to grasp the project as a whole.
- **Chapter 4 - Methodology:** The different technologies and instruments used in the

project are covered in this chapter. Fundamental physical principles which the instruments are based on are highlighted.

- **Chapter 5 - Immobilizing ligands on a surface:** The approach of immobilizing ligands on a surface in order to study a ligand-receptor interaction with single-event resolution is in this chapter motivated and further described in explicit experimental terms. Illustrations and output from a label-free sensing technique is added to emphasize the results of the immobilization step.
- **Chapter 6 - Fluorescent labeling of cell mimics:** Evaluation of three different alternatives for fluorescent labeling of vesicles containing the membrane receptor is covered in this chapter. Schematic illustrations and Total Internal Reflection Fluorescence Microscopy images forms the chapter.
- **Chapter 7 - Equilibrium fluctuation analysis:** The interaction between ligand and receptor is monitored in the microscope with a single molecule sensitivity under equilibrium conditions. Kinetic parameters characterizing the interaction are then extracted by image analysis.
- **Chapter 8 - Theoretical aspects:** A theoretical framework for determining characteristic parameters of a drug-receptor interaction is brought to light. Further aspects on how the setup can be developed are also treated.
- **Chapter 9 - Conclusions:** Experimental and theoretical insights gained in this project on determining kinetic parameters describing a ligand-receptor interaction under equilibrium conditions with a single molecule sensitivity are concluded in this section.
- **Chapter 10 - Future perspectives:** In this chapter future development of the method used in this project is treated. How can this equilibrium fluctuation analysis function as a platform for future drug development?

"An investment in knowledge pays the best interest."

Benjamin Franklin

2

Biological foundation

FUNDAMENTAL BIOLOGICAL STRUCTURES forming the basis of living organisms is covered in this chapter. Readers not in the field of biology or biological physics may find it helpful in order to keep up as the project progresses. First of all, life and its basic biological building blocks are enlightened. More complex structures within cells and the advantage of using cell mimics are then covered.

2.1 Life and its fundamental building blocks

Life and its origin is one of the most central topics in science. The highly motivated assignment to investigate and understand our own genesis is widely undertaken by many different science branches like biology, chemistry, physics, astronomy and mathematics. The mystery of life has engaged philosophers, theologians and scientists for two and a half thousand years and is still not fully unravelled.[7]

The earliest evidence for life are 3.4 billion-year-old fossils of sulphur-eating bacteria found in rocks in Australia [8]. At that time the living conditions on earth were harsh and inhospitable with a high volcanic activity, small atmospheric protection from the burning sun and very little oxygen. No highly complex life form like animals and humans would stand a chance to survive under those conditions. The origin of life is still today unknown, but there are several different theories.

Darwin deemed that life emerged from a warm puddle on the earth. However, more recent theories advocate that life originated from deep down below the surface of the earth or even from the outer space. Regarding the definition of life the common view is that there are certain physical criteria that needs to be fulfilled in order for a system to be considered alive. The two most important factors may be that a living system must consume energy and be able to reproduce itself [7, 9]. However, the latter criterion should not necessarily be applied on single individuals.

Another fundamental difference between living and dead systems is that living systems are built up by larger and structurally complex molecules, called macromolecules. There are four different classes of macromolecules forming the fundamental building blocks of all living organisms; proteins, carbohydrates, lipids and nucleic acids. They consist mainly of carbon (C), oxygen (O), nitrogen (N), hydrogen (H), sulphur (S) and phosphorus (P). These four classes of molecules serve different purposes in living systems. The proteins have many important functions in the cells, for example enzymes that catalyze chemical reactions. Carbohydrates are used for energy storage and may also have structural properties on the outside of the cell, as well as building up more rigid structures. Lipids, amphiphilic molecules with a hydrophilic head and a hydrophobic tail, build up the membrane structure that separates the cell from its surroundings. Lipid membranes also surround organelles inside the cell. The nucleic acids store all the genetic information and operating instructions.[9]

2.2 The cell membrane

The living cell is the smallest unit that is classified as alive and ranges in size from $1 - 100\ \mu m$ depending on type of cell, see figure 2.1. Furthermore, it is considered to be the most complex system of that size that we know of [7]. Since this project focuses on ligand-receptor interactions between potential drug molecules and membrane proteins the entire cell machinery and crowded interior of the cell is not further treated. Instead focus will be on the cell membrane and mimics of it. The next chapter will focus on the fundamental concept of ligand-receptor interactions.

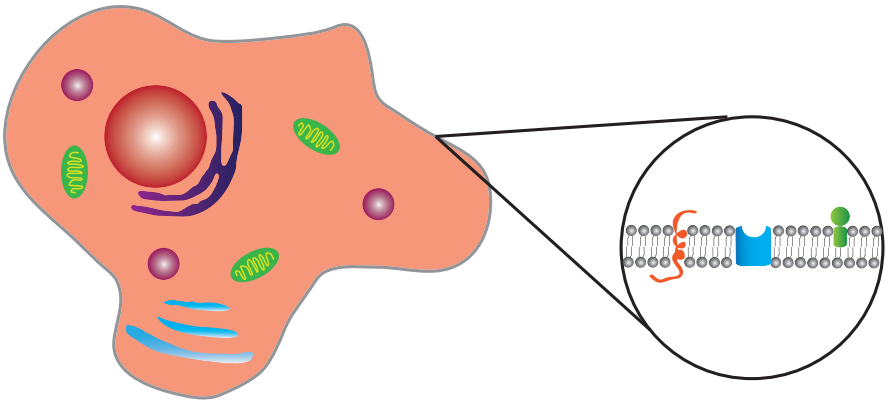

Figure 2.1: *An illustration of an eukaryotic cell, with cell nucleus and other typical organelles such as the golgi apparatus, lysosomes, endoplasmatic reticulum and mitochondria. Magnified is the cell membrane showing different types of incorporated proteins, so called membrane proteins.*

Membranes have been of great importance in the formation of life. The membrane serves as a barrier to maintain differences in chemical compositions between the cell interior and exterior. It must however allow some transport through it in order for the cell to get nutrients and get rid of waste products. Additional demands are that the membrane must be stretchable to enable cell movement, growth and division. One clever way of designing such a membrane is to use building blocks with two distinct physical properties. [9]

The amphiphilic phospholipid is the basic building block of cell membranes. The Greek *am-*

phis means both and *philia* means love. The molecule has both a water-loving (hydrophilic) part and one fat-loving (hydrophobic). These two properties are fundamental for molecules forming membranes. To minimize the free energy when dissolved in an aqueous solution the hydrophilic heads screen the hydrophobic tails and aggregates are formed spontaneously, which is referred to as the hydrophobic effect [10]. The optimum head-group area, critical chain-length and hydrocarbon volume of the amphiphilic molecules are parameters that determine how the lipid molecules aggregate [11]. The two types of aggregates relevant for this project is the lipid vesicle and the supported lipid bilayer, shown in figure 2.2. [9]

The cell membrane contains many different types of lipids but also several different proteins with a variety of purposes. In 1972, Singer and Nicolson proposed that the cell membrane can be seen as a two-dimensional fluid of oriented lipids and proteins [12]. This so called fluid mosaic model had a great influence on the understanding of membrane topology. However, in 1982, Karnovsky et al. showed that the movement of some membrane proteins was constrained, leading the way to the concept of lipid rafts [13].

2.3 Mimicing a simplified nature

In order to study complex processes occurring naturally inside our bodies simplifications of ingoing biological systems are of vital importance. Biological structures must both be compatible with actual techniques used for studying and it is an advantage if the studied entity or process can be isolated from inflicting factors. Furthermore, being able to give the simplified model system a theoretical foundation may increase the relevance of experimental results.

In this project two common cell membrane mimics have been used. The lipid vesicle and the supported lipid bilayer. Lipid vesicles, illustrated in figure 2.2b, are formed spontaneously via self-assembly when lipids, figure 2.2a, are dissolved in an aqueous solution. A supported lipid bilayer, illustrated in figure 2.2c, is formed spontaneously via vesicle adsorption on only a few hydrophilic supports, one example is SiO_2 [14]. When the vesicle coverage reaches a certain critical value the vesicles rupture and form a lipid bilayer on the support. Variations in how these aggregates are formed exist due to varying physical properties of different lipids and surfaces.

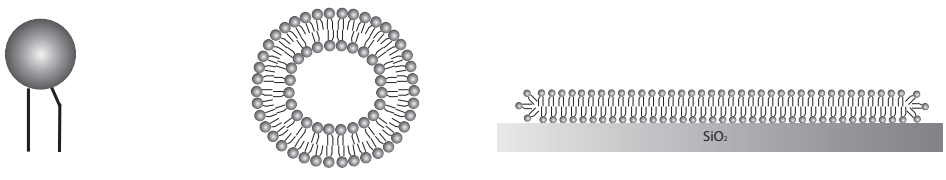

(a) **(b)** **(c)**

Figure 2.2: *A lipid molecule* ***(a)*** *has a hydrophilic head and a hydrophobic tail(s). This amphiphilic nature of lipid molecules is responsible for the self assembly of lipid structures into lipid vesicles* ***(b)*** *and bilayers on some solid supports* ***(c)****.*

"A biophysicist talks physics to the biologists and biology to the physicists."

Author Unknown

3

Pharmacodynamics

PHARMACOLOGY as a science started to develop into the form we know of in the middle of the 1800's. Etymologically, pharmacology means the science of drugs from the Greek *pharmakos* for medicine or drug, and *logia*, study of. It covers the effect of chemically acting substances on living organisms and is a good example of where cooperation between multiple science disciplines facilitates acquirement of deeper insights and revolutionizing ideas. [15]

Pharmacodynamics and pharmacokinetics are both branches of pharmacology. The former describes the biochemical and physiological effect of drugs on the body while the latter is related to the reverse; how biological systems affect drugs. In this project, where the interaction between drugs and membrane proteins is investigated, pharmacodynamics is the science branch to recall. The suffix *dynamic* is also Greek and relates to power and strength.

3.1 Ligand-receptor interaction

The reaction studied in this project is how a chemokine ligand (CXCL10) binds to a GPCR (CXCR3) that resides in the cell membrane. The terminology related to the interaction between a ligand and a receptor is often founded with a basic cartoon. To stick to the usual way of introducing pharmacologically relevant terminology, figure 3.1 is first out to illustrate the binding of a ligand (L) to a receptor (R), forming the complex (LR). While this complex is activated, (LR*), a physiological response is provided [16].

k_{on} is the rate at which ligands (L) bind to receptors (R) and form a complex (LR). Similarly, k_{off} is the rate at which ligands unbind from receptors. The rates are governed by the affinity of the ligand to the receptor. Furthermore, the rate at which the complex activates (LR*) is β, and deactivates α. These rates are governed by the efficacy. Since this project focuses on measuring the affinity of potential drugs, the activation/deactivation of ligand-receptor complex is not further treated.

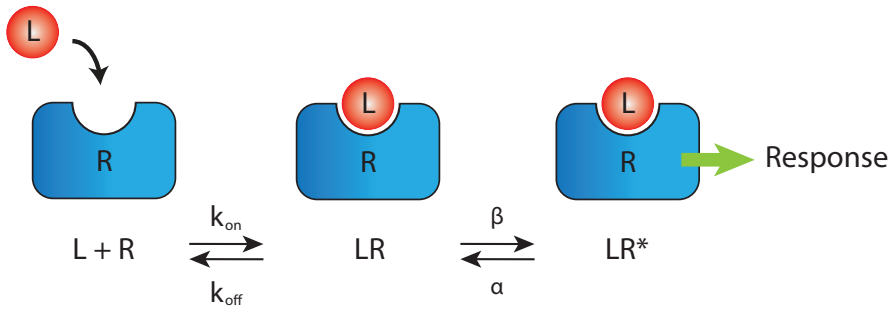

Figure 3.1: *An illustration of the interaction between a ligand (L) and receptor (R). The rates k_{on} and k_{off} describes the tendency of a ligand to bind/unbind from the receptor. Similarly, the rates α and β describes the tendency of the ligand-receptor complex to deactivate/activate. Only an active complex can provide a response.*

A deeper interpretation of the formation of a complex between ligand and receptor is elaborated by adding a step in the association between ligand (L) and receptor (R) [17]. Compare the first step in figure 3.1 with equation (3.1).

$$L + R \underset{d_-}{\overset{d_+}{\rightleftarrows}} (L - R) \underset{r_-}{\overset{r_+}{\rightleftarrows}} LR \tag{3.1}$$

where the first step describes the formation of an encounter complex, (L-R), and the second step represents a bond formation. The kinetic parameters, k_{on} and k_{off}, describing the relationship between $[L + R]$ and $[LR]$ are now obtained by expressing $d[LR]/dt$ in terms of $[L-R]$ and $[LR]$. By assuming that the concentration of the encounter complex is stationary, i.e. $d[L - R]/dt = 0$ [17], the kinetic parameters can be expressed as

$$\begin{aligned} k_{on} &= \frac{d_+ r_+}{d_- + r_+} \\ k_{off} &= \frac{d_- r_-}{d_- + r_+} \end{aligned} \tag{3.2}$$

Describing the association between ligand and receptor in two separate steps is not part of the experimental and analyzing part of this project. However, in the theoretical view of the ligand-receptor interactions presented later, this added step is incorporated. To get a more extensive view on the characterization of a potential drug candidate some further theoretical calculations will be made, recalling the Langmuir model.

3.2 The Langmuir model

By immobilizing either the ligands or the receptors on a surface the Langmuir theory can be applied, describing how adsorption of molecules on a surface relates to pressure or molecular concentration. In this project the ligands are immobilized. The nomenclature is that $\Theta(t)$ is the time-dependent number of ligands bound to a receptor. Θ_{max} is the total number of

ligands on the surface. $\Theta(t)/\Theta_{max}$ is thus the fraction of ligands that have a receptor bound to them, referred to as the relative surface coverage.

By adding receptors in a solution above a surface with immobilized ligands and monitor the fraction of ligands attached to a receptor something that looks like figure 3.2 is received. An equilibrium is reached when the coverage is so high that receptors associate and dissociate with equal speed. The coverage decreases exponentially upon rinsing. From this measurement the kinetic parameters k_{on} and k_{off} can be extracted.

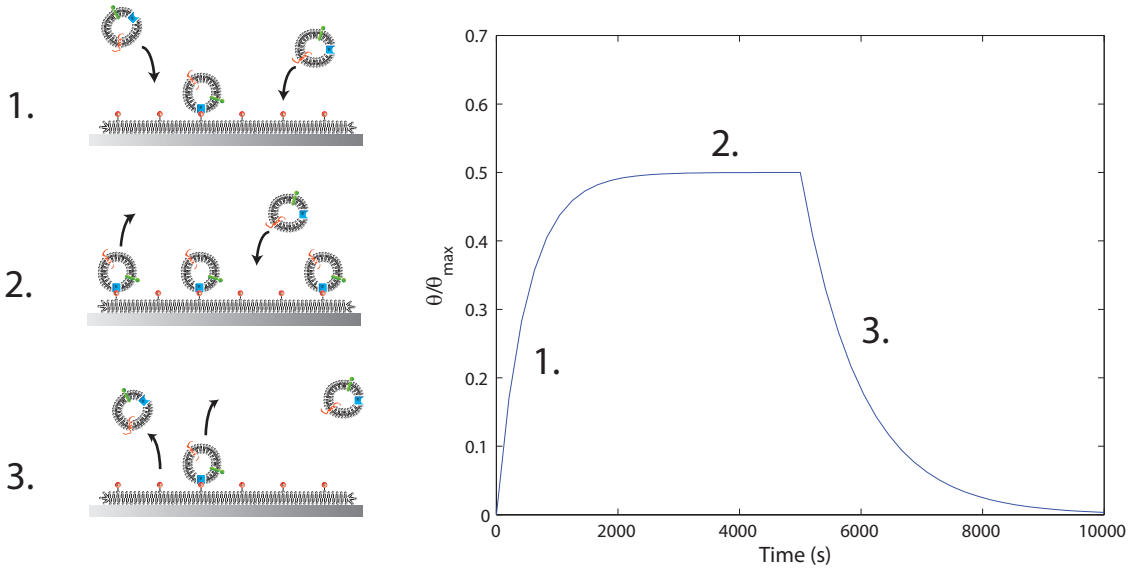

Figure 3.2: *Illustrated is the relative surface coverage of receptors on ligands as a function of time. At time zero vesicles containing receptors are injected above the surface with immobilized ligands.* ***(1)*** *The relative surface coverage increases as more and more receptors attach.* ***(2)*** *An equilibrium is reached when the rates at which receptors attach and detach are equal, which results in a constant surface coverage.* ***(3)*** *Rinsing occurs after* 5000 *s, which makes the relative surface coverage decrease exponentially.*

k_{on} and k_{off} are the rates at which receptors bind and unbind the ligands. With the law of mass action, that describes the rate of chemical reactions, the behaviour of such a system can be written as a differential equation.

$$\frac{d\Theta(t)}{dt} = k_{on}C(\Theta_{max} - \Theta(t)) - k_{off}\Theta(t) \tag{3.3}$$

where C refers to the receptor concentration in the solution, i.e. the bulk. The evolution of the system in time is given by the solution to this first order non-homogeneous differential equation. The solution is found by first separating the equation into one part including terms of $\Theta(t)$ and its derivatives while the other part contains remaining terms.

$$\frac{d\Theta(t)}{dt} + \Theta(t)(k_{on}C + k_{off}) = k_{on}C\Theta_{max} \tag{3.4}$$

The course of action is then to rewrite the left side to a derivative by multiplying both sides with an integrating factor, $\sigma(t)$, by applying the chain rule. In this case $\sigma(t) = e^{(k_{on}C+k_{off})t}$, which yields

$$\frac{d}{dt}\left(e^{(k_{on}C+k_{off})t}\Theta(t)\right) = k_{on}C\Theta_{max}e^{(k_{on}C+k_{off})t} \tag{3.5}$$

Both sides are then integrated and by inserting the initial condition that the surface coverage is zero at time zero, i.e. $\Theta(0) = 0$, the solution obtained is

$$\Theta(t) = \frac{k_{on}C\Theta_{max}}{k_{on}C + k_{off}}\left(1 - e^{-(k_{on}C+k_{off})t}\right) \tag{3.6}$$

By letting t $\to \infty$ the fractional coverage $\Theta(t)/\Theta_{max}$ converges and reaches an equilibrium. This equilibrium coverage can be written as

$$\frac{\Theta(t)}{\Theta_{max}} = \frac{k_{on}C}{k_{on}C + k_{off}} = \frac{C}{C + K_d} \tag{3.7}$$

This result is known as the Hill-Langmuir equation, where K_d is defined as k_{off}/k_{on} and is interpreted as the concentration resulting in a relative coverage of 0.5 at equilibrium.

Equation (3.6) is illustrated for three different receptor concentrations in figure 3.3a and equation (3.7) in figure 3.3b.

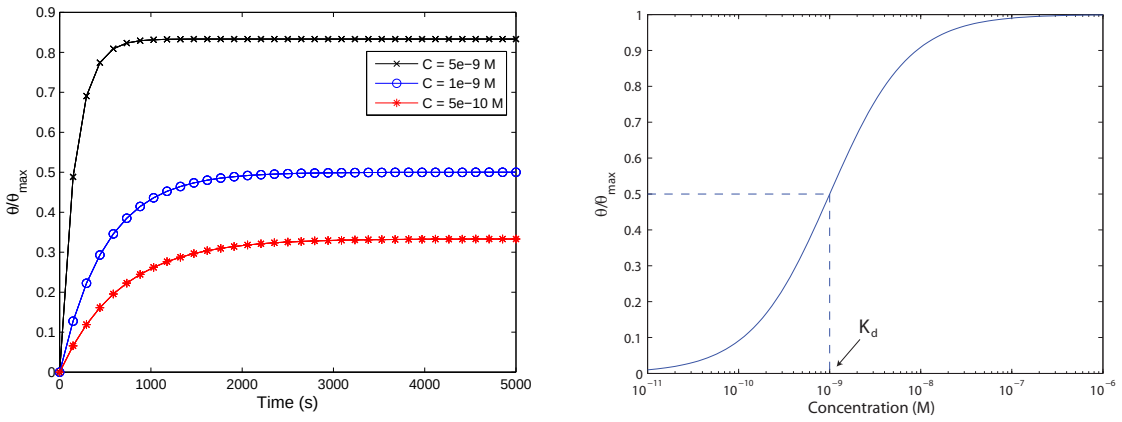

(a) **(b)**

Figure 3.3: ***(a)*** *Fraction of ligands bound to a receptor as a function of time for three different concentrations. k_{on} is set to $10^6\ s^{-1}M^{-1}$, and k_{off} is set to $10^{-3}\ s^{-1}$.* ***(b)*** *Fraction of ligands bound to a receptor at equilibrium as a function of concentration of receptors in the bulk. The dashed lines emphasize the equilibrium dissociation constant, K_d, which is the concentration that results in a half maximum surface coverage at equilibrium. Kinetic parameters are the same as in (a).*

3.3 Inhibition by an antagonist

Another fundamental concept in pharmacology, occurring naturally, is inhibition. That is when another ligand, so called antagonist, binds to receptors and blocks the main ligand-receptor interaction, without providing a physiological response. An example is *propranolol* blocking the binding of *noradrenaline* to β-Adrenoceptors, which mediates the fight-or-flight response [16]. The process is shown in figure 3.4. This concept can be used for studying the kinetic parameters of the ligand-receptor interaction.

While having the receptors in a solution above the immobilized ligands, which is the approach in this project, an added antagonist can reduce the effective concentration of receptor molecules in the solution. A receptor will not be able to bind to the surface if it already has a ligand bound to it. In addition, the ligand itself can act as an antagonist, since the purpose is to prevent some receptors from being able to interact with the immobilized ligands. In this way the effective receptor concentration can easily be tuned without undesirable steps of addition and removal of different solutions enabling explicit determination of the equilibrium dissociation constant, K_d.

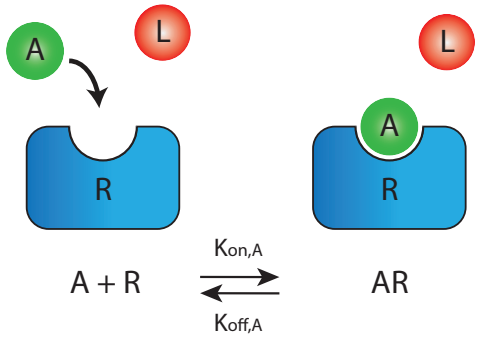

Figure 3.4: *An illustration of the interaction between an antagonist (A) and a receptor (R). The rates $k_{on,A}$ and $k_{off,A}$ now describes the tendency of the antagonist to bind/unbind from the receptor. The antagonist prevents the receptor from binding to immobilized ligands reducing the effective concentration of receptors in bulk.*

"All of physics is either impossible or trivial. It is impossible until you understand it, and then it becomes trivial."

Ernest Rutherford

4

Methodology

The fundamental steps leading to the sought after characterization of potential drugs involves several different instruments and techniques originating from various scientific disciplines. The techniques used in this project are fundamentally different from conventional techniques used for drug discovery and screening such as SPR [18], crystallography [19] and radioligand assays [20]. This chapter gives a brief explanation to each of the techniques playing a key role in this project. Basic experiments will illustrate the output of the different instruments, shown in figure 4.1.

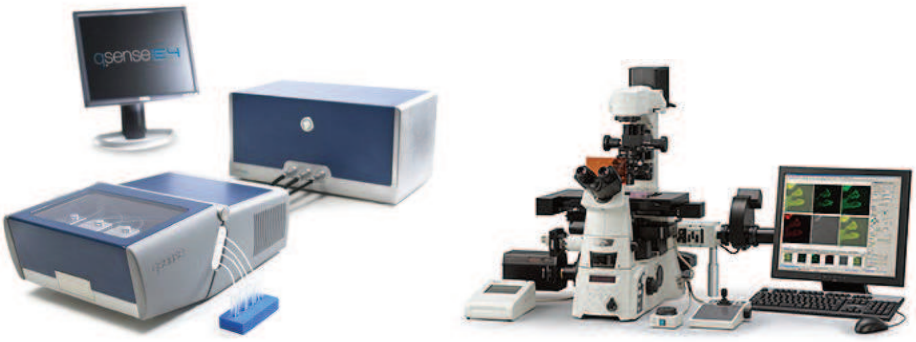

(a) **(b)**

Figure 4.1: *The two different instruments mainly used in the project.* ***(a)*** *A Q-Sense E4 instrument based on the Quartz Crystal Microbalance with Dissipation monitoring technique. Image from* `q-sense.com`*.* ***(b)*** *A Nikon Ti Eclipse microscope with Total Internal Reflection Fluorescence Microscopy. Image from* `nikon.com`*.*

4.1 Quartz Crystal Microbalance with Dissipation monitoring - QCMD

QCMD is an acoustic biosensing technique that allows for label-free high-sensitivity studies of adsorption and interaction of molecules on various surfaces. The mass adsorbed on the surface can be measured with a sensitivity of up to $1\,ng/cm^2$ and the technique can be applied on biological and chemical entities ranging in weight from less than $200\,Da$ to that of an entire cell, which is of the order of GDa [21]. Structural parameters like elasticity and viscosity can also be modeled from the measurements.

The basis of the sensor is the piezoelectric property of quartz. When exposed to an external electric field the quartz crystal deforms. Similarly, an electric field is generated when the crystal is deformed. This phenomenon is due to spontaneous alignment of electric dipoles within small subdomains of the crystal [22]. By applying an alternating voltage to an appropriately cut crystal it will start to oscillate in a shear fashion with a certain resonance frequency. The Sauerbrey relation, which states that there is a linear relationship between adsorbed mass and shift in resonance frequency of the crystal, is the bridge between measurements and results. [21]

$$\Delta m = -\frac{C\Delta f}{n} \tag{4.1}$$

where Δm is the change in adsorbed mass per area unit and Δf is the change in resonance frequency. $C = 17.7\ ng/(Hz\ cm^2)$ for a $5\ MHz$ crystal [14] and n is the number of the odd harmonic used. The relation holds for rigid, evenly distributed and sufficiently thin adsorbed layers of molecules. When an adsorbed layer does not fulfil these requirements the Sauerbrey relation underestimates the mass of the layer. By combining information on frequency shift and dissipation from multiple harmonics with viscoelastic models, the thickness, shear elastic modulus, and viscosity of the adsorbed film can be estimated. This contributes to the characterization of the adsorbed layer even though it is out of the Sauerbrey regime. Figure 4.2a shows a schematic illustration of the setup and how the quartz crystal oscillates. Figure 4.2b shows the quartz crystal used as the sensing element from a top view.

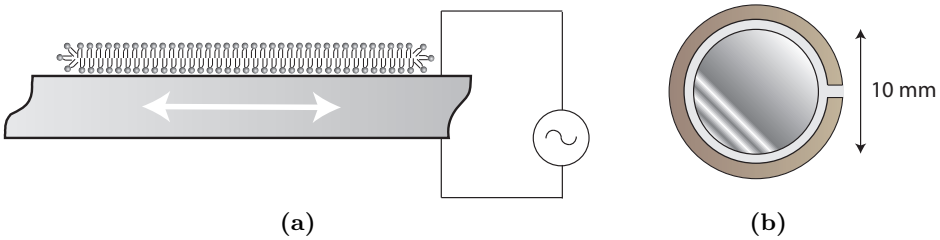

Figure 4.2: ***(a)*** *A schematic illustration of a QCMD. An alternating voltage makes the quartz crystal oscillate in a shear fashion as the double arrow indicates. When an odd multiple of $\lambda/2$ of the acoustic wave created matches the thickness of the crystal the resonance condition is fulfilled.* ***(b)*** *A quartz crystal used as the sensing platform in QCMD seen from above.*

An alternating voltage excites the quartz crystal via two gold electrodes, one on either side of the crystal. The fundamental frequency corresponds to the situation when $\lambda/2$ of the acoustic wave created equals the thickness of the crystal. The harmonics are odd multiples of the fundamental frequency. By monitoring the change in resonance frequency and the dissipation of energy in the oscillations the mass and viscoelastic properties of adsorbed molecular layers can be obtained in real time. The dissipation is a measure on how much energy that is lost from the system in one oscillation cycle. The quantity is dimensionless and defined as

$$D = \frac{E_{lost}}{2\pi E_{stored}} \tag{4.2}$$

where E_{lost} is the energy dissipated from the system during one oscillation cycle and E_{stored} is the total energy stored in the system. [23]

The QCMD was used in this project for evaluating different coupling chemistries for immobilizing the ligands on a surface and to find conditions that reduce the so called unspecific binding of vesicles containing receptors to the surrounding surface. One major drawback with the QCMD is the high material consumption. It is recommended not to use volumes smaller than 150 μl [24]. However, by adding samples to the surface in a batch-mode fashion, where the pump runs slowly ($\sim 25 \mu l/min$) or even stopped when the sample has reached the crystal, smaller volumes are possible to use but far from optimal.

When the desired surface chemistry for immobilization of the ligands was found it could be implemented and used for the equilibrium fluctuation analysis [3] using a fluorescence microscopy setup.

4.1.1 Bilayer formation in QCMD

To provide a better feeling for the output of the instrument a basic experiment is presented, in which a bilayer is being formed when vesicles adsorb to the SiO_2-coated surface of quartz, see figure 4.3. A bilayer is used in this project to mediate the immobilization of ligands to a surface as well as reducing the unspecific binding to the surface by its so called inertness. Vesicles consisting of POPC lipids solved in PBS buffer are used. The frequency decreases as more and more vesicles attach to the crystal surface. The dissipation however increases because the vesicles effectively damp the oscillation of the crystal. When the vesicles cover a certain critical fraction of the crystal surface they begin to rupture and fuse into a bilayer. The frequency now increases because the buffer inside and between the vesicles no longer contributes to the coupled mass. The dissipation decreases, which is because a bilayer is thinner and more rigid than the corresponding number of non-ruptured vesicles attached to the surface. Figure 4.3 shows the frequency shift (Δf) and the dissipation shift (ΔD) for harmonic 3,5,7,9 and 11 as a function of time as the bilayer is formed. Note that the bilayer formed has a weight that corresponds to a frequency shift of about $-25\,Hz$ and a dissipation shift around $0.5 \cdot 10^{-6}$.

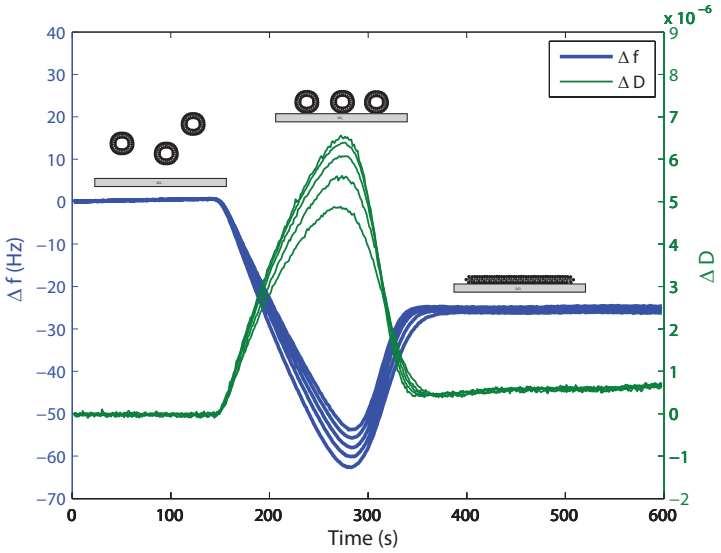

Figure 4.3: *A QMCD plot showing the formation of a bilayer. The thicker blue curves show frequency shift (Δf) in Hz for the harmonics 3,5,7,9 and 11. Green thinner curves show dissipation shift (ΔD) for the same harmonics. The baselines, where both the frequency and dissipation shift is zero, are recorded with PBS buffer flowing over the crystal surface. At 150 s POPC vesicles of concentration $0.1\,mg/ml$ solved in PBS reaches the crystal surface. The frequency drops gradually as more and more vesicles attach to the surface of the crystal. The dissipation increases, which is a consequence of the vesicles dampening the oscillations. The separation of the different curves at this stage is due to the fact that the layer adsorbed on the crystal surface is thick and non-rigid, and thus out of the Sauerbrey regime. At a certain surface coverage the vesicles rupture and form a bilayer. The frequency shift increases because the mass of the buffer inside the vesicles no longer couples to the crystal. Likewise, the dissipation decreases because the bilayer is thinner and more rigid than single vesicles attached to the surface.*

4.2 Total Internal Reflection Fluorescence Microscopy - TIRFM

To be able to study separate interactions between molecules of nanometer size taking place on a surface an optical setup involving fluorescence is a very powerful tool. However, in a regular fluorescence microscope not only the fluorescent molecules attached to the surface are visible, but also those present further away in the liquid medium above the substrate, the so called bulk. This results in a substantial background signal that makes it difficult to distinguish separate binding events on the surface. In 1981 Daniel Axelrod, at the University of Michigan, developed a technique that enabled selective illumination of only the fluorescent molecules close to the substrate-liquid interface [25]. The basis for the new technique was light being totally reflected at the interface between substrate and liquid. Under these conditions an exponentially decaying electromagnetic field extends into the liquid medium.

This so called evanescent field confines the excitation of fluorescent molecules to a small volume extending only about one wavelength from the substrate surface. Thus, the background signal is substantially reduced which enables studies of single binding/unbinding events.[25]

The basis of the total internal reflection microscope is the refraction of light travelling between mediums with different optical densities. The refraction of a certain beam of light is governed

by Snell's law

$$n_1 \sin(\theta_1) = n_2 \sin(\theta_2) \tag{4.3}$$

where n_1 and n_2 denotes the refractive indices of the two mediums respectively. θ_1 and θ_2 denotes the angles between the normal to the surface and the direction of the beam in each medium according to the indices, see figure 4.4.

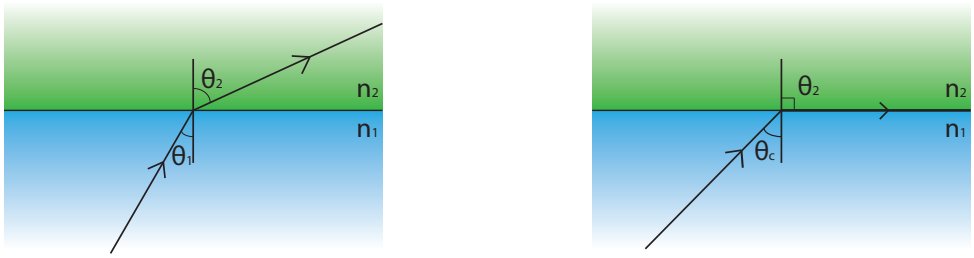

(a) **(b)**

Figure 4.4: *Illustration of two different beams travelling from an optically denser medium (1) to a less dense medium (2).* ***(a)*** *The beam is refracted away from the normal line since $n_2 < n_1$.* ***(b)*** *When the incident angle is further increased it will reach a critical value θ_c, which results in a refraction angle, θ_2, of 90^o. This is the total internal reflection limit. If the incident angle is further increased the beam will be reflected.*

If light travels from an optically denser to a less dense medium and the angle of incidence is increasing, a point will be reached where the refraction angle becomes 90^o, see figure 4.4b. The angle at which this occurs is termed the critical angle, θ_c, and is defined as

$$\theta_c = \arcsin(\frac{n_2}{n_1}) \tag{4.4}$$

If the angle of incidence is further increased the light will be reflected instead of refracted. Even though light is not transmitted through the interface an electromagnetic field appears in the optically less dense medium called an evanescent field. The intensity of the evanescent field decays exponentially with distance from the interface according to

$$I(z) = I(0) \exp(-z/\delta) \tag{4.5}$$

where z is the distance away from the interface, I(0) is the intensity at the interface and δ is the decay constant defined as

$$\delta = \frac{\lambda}{4\pi n_2} \left(\frac{\sin^2 \theta}{\sin^2 \theta_c} - 1 \right)^{-1/2} \tag{4.6}$$

where λ is the wavelength of the light, n_2 is the refractive index of the liquid medium, θ is the angle if incidence and θ_c is the critical angle [25].

A schematic illustration of a TIRF-setup is seen in figure 4.5, where fluorescent particles that reside close to the substrate are excited by the evanescent field and emit light.

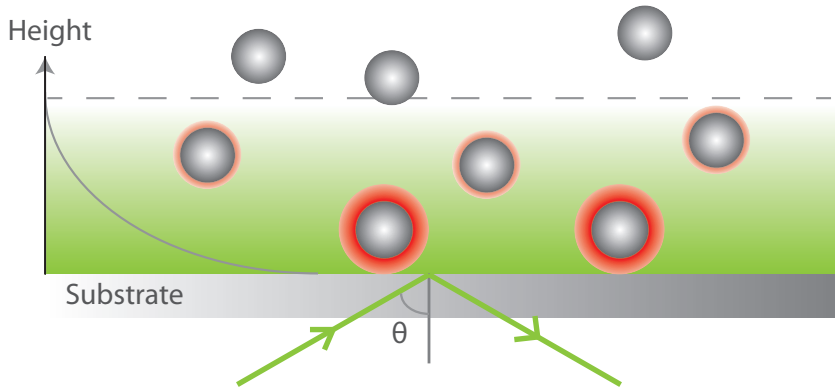

Figure 4.5: *An illustration of the basics of Total Internal Reflection Fluorescence Microscopy. Light is totally reflected in the interface between substrate and liquid. An exponentially decaying evanescent field extends a few hundred nanometers above the substrate. Only the fluorescent particles that reside in the volume where the evanescent field is present are excited.*

4.2.1 Bilayer formation in TIRFM

Again, an illustrative demonstration of the technique previously described is the formation of a bilayer on a SiO_2 surface. Vesicles consisting of POPC, biotin-DOPE and rhodamine-DOPE with a concentration of $10\,\mu g/ml$ solved in PBS were added to a clean microtiter-plate well. Snapshots were taken every $2\ s$ with the TIRF microscope.

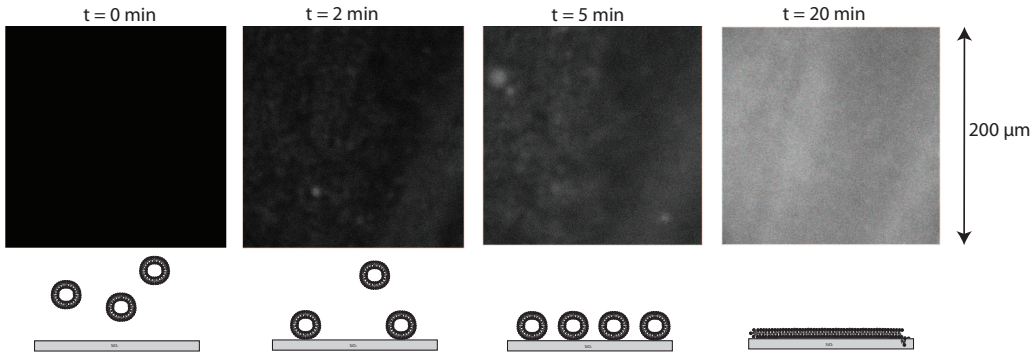

Figure 4.6: *Illustrations and TIRF snapshots of the formation of a bilayer in a microtiter well. Vesicles of POPC, biotin-DOPE and rhodamine-DOPE with concentration $10\,\mu g/ml$ were injected at $t = 0$. The fluorescent signal increases as more and more vesicles attach to the surface. When the surface coverage reaches a certain critical fraction the vesicles start to rupture and fuse together into a bilayer. The time-scale of the formation is indicated above the snapshots. The width of one frame is $\approx 200\mu m$.*

"Science is organized knowledge.
Wisdom is organized life."
Immanuel Kant

5

Immobilizing ligands on a surface

To study the interaction between a ligand and a transmembrane receptor is a non-trivial and highly delicate problem. First of all, the interaction must be detected in some way to be characterized. Another requirement on the setup is that it has to represent the actual situation inside the body, i.e. *in vivo*, or made in a way such that it is possible to adjust or back-calculate the results from the experiments to obtain information about what happens in reality. The different steps taken in this project towards characterizing ligand-receptor interactions will be covered in this and the following two chapters. The fundamental approach and its justification will first be treated.

One crucial part of the setup for studying the interaction between a ligand molecule and a membrane protein receptor is that the membrane protein is kept in an environment that is similar to its natural. This is required in order for it to function properly. Therefore, it is not desirable to immobilize single membrane proteins directly on a surface. This situation will not coincide with its natural environment, where the two outer ends are in contact with liquid and the center part is embedded in the cell membrane. The protein will likely denature and stop function. The desired approach would then be to let the membrane protein stay incorporated in a cell membrane, which is its natural environment, and instead immobilize the ligand on the surface. In this project vesicles derived directly from membranes of cells expressing the certain membrane protein (CXCR3) are used. The diameter of the vesicles was measured with a nanoparticle tracking analysis instrument to $250\,nm \pm 150\,nm$, with each vesicle containing about one CXCR3 receptor on average.

Furthermore, unspecific interactions between the receptor containing vesicles and the surface is undesired. The surface needs to be made so called inert. This is often realized by forming the connection chemistry relevant for the ligand-receptor pair on top of either a lipid bilayer or a layer of polymers. The foundation will serve as a medium where few receptor-containing vesicles will attach, which reduces the number of unspecific binding events and thus facilitates further studies. Irreversibility of the connection between ligand and the foundation medium is another desirable feature to not interfere with the study of the interaction between ligand and receptor, which is reversible.

5.1 CXCL10 immobilized on POPC-bilayer

The molecule that was used as a ligand was the CXCL10, which is a small ($\sim 9\,kDa$) protein belonging to a group of proteins called chemokines. The chemokines promote recruitment and activation of leukocytes, making them to an important part of the immune system [26]. The CXCL10 was immobilized using a lipid bilayer as a foundation for the purpose of inertness. To evaluate whether the vesicles containing the CXCR3 receptors bound the immobilized CXCL10 ligand QCMD experiments were performed.

The CXCL10 protein was immobilized on a lipid bilayer consisting of 10wt% maleimide-functionalized DOPE-lipids (MCC-DOPE), 70wt% POPC-lipids and 20wt% cholesterol for stability. Traut's reagent was used for forming the bond between CXCL10 and maleimide. An amine group (NH_2) of the CXCL10 forms together with Traut's reagent a sulfhydryl-modified molecule. The sulhydryl group (SH) binds covalently to the maleimide group on the surface. The functionalized bilayer mediates the relevant ligand-receptor connection and makes the surface inert. Figure 5.1 illustrates in detail how the CXCL10 molecules are immobilized on the maleimide groups on the bilayer using Traut's reagent.

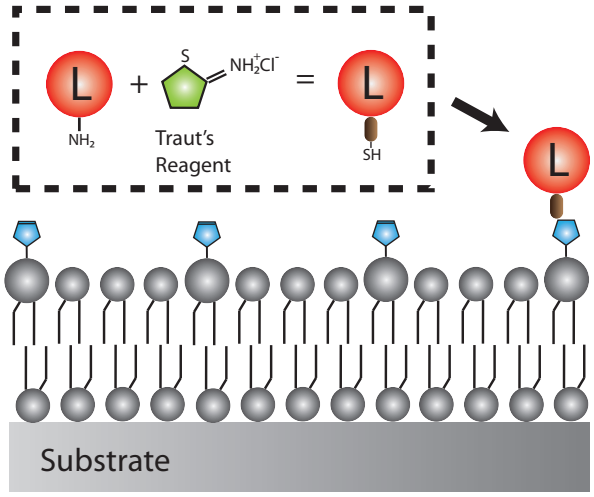

Figure 5.1: *An illustration of how CXCL10 (L) is immobilized on a bilayer functionalized with maleimide groups (blue pentagons). Traut's reagent (green pentagon) forms together with an amine group (NH_2) part of CXCL10 a sulfhydryl group (SH). This sulfhydryl group can then bind covalently to a maleimide group on a DOPE-lipid in the bilayer immobilizing the ligand on the surface.*

The surface chemistry was evaluated with QCMD. Vesicles containing the CXCR3 receptor were injected to both a positive control with immobilized ligands on a bilayer and a negative control with only a bilayer functionalized with maleimide groups. Corresponding QCMD curve with illustrations is seen in figure 5.2, which clearly shows specific binding of vesicles containing the CXCR3 receptor to the immobilized CXCL10 molecules.

Now, when the coupling chemistry for immobilization of ligands on a bilayer is confirmed a way of fluorescently label the vesicles containing the CXCR3 receptor needs to be found. This

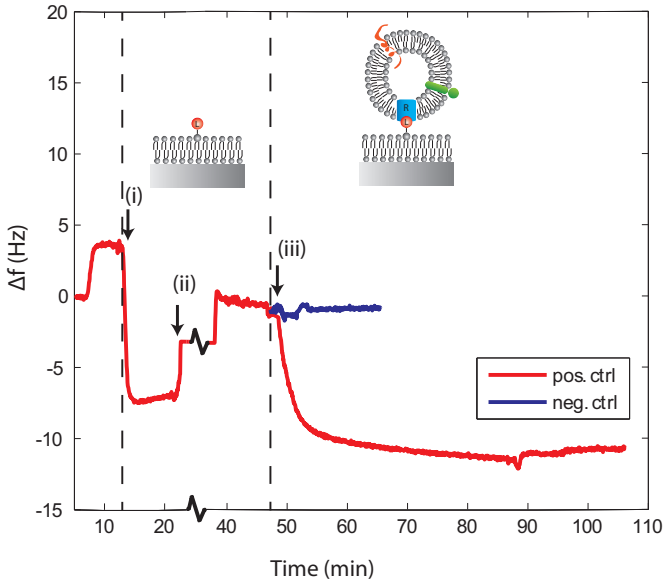

Figure 5.2: *QCMD-plot and illustrations showing the immobilization of CXCL10 and the specific binding of CXCR3 containing vesicles.* ***(i)*** *Injection of CXCL10 incubated in Traut's reagent.* ***(ii)*** *Rinse with NaAc buffer.* ***(iii)*** *Injection of vesicles containing the CXCR3 receptor. The negative control, without immobilized CXCL10, shows a modest binding of vesicles leading to the conclusion that the CXCR3 receptor binds specifically to CXCL10.*

is in order to see the interaction between ligand and receptor in the fluorescence microscope enabling equilibrium fluctuation analysis with a single molecule resolution.

"Measure what is measurable, and make measurable what is not so."
Galileo Galilei

6

Fluorescent labeling of cell mimics

Characterizing ligand-receptor interactions with a single molecule resolution enables studies of membrane proteins, potentially without the additional steps of over-expression making this method interesting for pharmaceutical industry. The proteins can be kept in a natural environment which better represents the *in vivo* situation. Single molecule resolution also enables extraction of kinetic parameters at equilibrium, which further simplifies the analysis since additional injection and rinsing steps are eliminated.

The approach is to visualize single interactions between ligands and receptors using fluorescence. The vesicles containing the membrane protein needs to be labeled with fluorescent molecules to be visible in the TIRF microscope. These molecules are incorporated into the membrane of the vesicles and will only be excited when residing in close proximity of the surface, where the evanescent field as well as the ligands are present. This is what makes it possible to get information about the interaction between ligand and receptor.

Three different dyes were evaluated for labeling of the vesicles containing the membrane protein, see figure 6.1b. It must be possible to incorporate a sufficient amount of fluorescent molecules into the membrane of the vesicles in order to make it visible in the microscope. Furthermore, transfer of the fluorescent labels to the bilayer where the ligands are immobilized is undesirable since an increased background signal reduces the signal-to-noise making binding/unbinding events more difficult to distinguish with the image analysis software. For the evaluation of the different dyes, pure POPC-bilayers were formed in microtiter wells, see figure 6.1. Vesicles containing the receptor labeled with the different dyes were added to separate wells and the acquisitions were performed with the microscope for about 30 minutes.

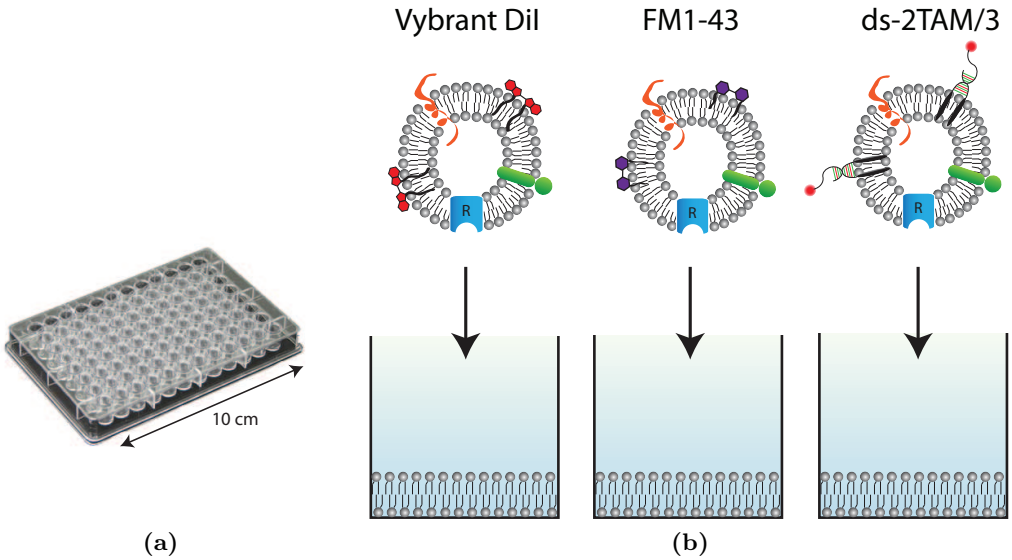

Figure 6.1: ***(a)*** *A 96 well microtiter plate. The illumination and objective is underneath the well. Picture from* `bio-world.com`*.* ***(b)*** *Illustration of the evaluation of the three different dyes. The vesicles containing the CXCR3 receptor (R) are labeled with the three dyes and added to microtiter wells prepared with bilayers of POPC. Vybrant DiI (red polygons), FM1-43 (purple hexagons) and ds-2TAM/3 (two complementary DNA strands anchored by two cholesterol molecules having a rhodamine molecule at the end of the longer strand) are incorporated into the vesicle membrane.*

6.1 Vybrant DiI and FM1-43

Two commercially available cell-stain solutions were evaluated in the TIRF microscope, Vybrant DiI and FM1-43, see figure 6.1b. Vesicles containing the CXCR3 receptor were incubated with the two different dyes and added to microtiter wells prepared with a POPC-bilayer in order to study the visibility of the vesicles and the label-transfer. The results are shown in figure 6.2 and 6.3.

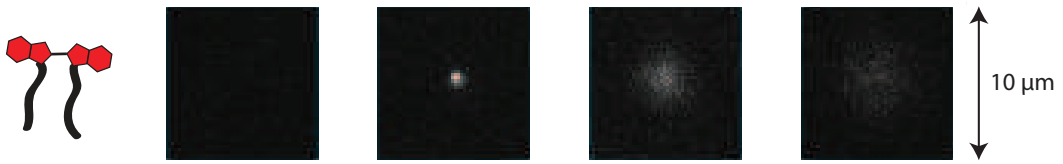

Figure 6.2: *Four pictures showing the transfer of Vybrant DiI from vesicles dyed with these molecules to a POPC-bilayer. At first no vesicle has attached to the area shown. Then a vesicle adsorbs to the surface and almost all fluorescent molecules are transferred. Something analogous to a footprint of fluorescent molecules is seen after vesicle detachment. The fluorescent molecules then diffuse around in the bilayer, which makes the imprint less distinct with time. The width of one frame is* $\approx 10\,\mu m$*. The time between the frames is of the order of minutes.*

Both the Vybrant DiI and the FM1-43 showed considerable label-transfer even though spin-columns were used to get rid of excess dye not incorporated into the membrane. However,

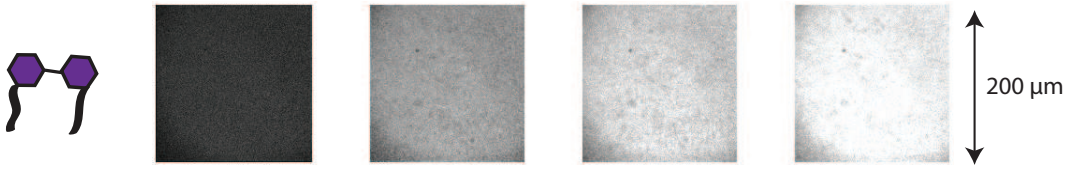

Figure 6.3: *Four pictures showing the transfer of FM1-43 from vesicles dyed with these molecules to a POPC-bilayer. The background intensity increases continuously and in a more uniform fashion unlike the Vybrant DiI. The width of one frame is* $\approx 200\ \mu m$*. The time between the frames is of the order of minutes.*

the label-transfer did not occur in the same way for the different dyes. For the Vybrant DiI it seemed that dye was only transferred when vesicles were in contact with the bilayer. For the FM1-43 on the other hand a continuous increase in fluorescence of the background was observed. A low affinity of the dye molecules to the vesicle membrane leading to a considerable transfer to the bilayer could be the reason.

6.2 ds-2TAM/3

The third alternative for labeling the CXCR3 containing vesicles was to use the ds-2TAM/3, which is two complementary DNA strands of different length ($12 + 27\,bps$). The longer strand has a rhodamine molecule attached to it, which is fluorescent. The strands are connected to two cholesterol molecules for irreversible anchoring into the vesicle membrane, see figure 6.1b. The result when adding vesicles incubated with this dye to a microtiter well prepared with a POPC-bilayer is seen in figure 6.4.

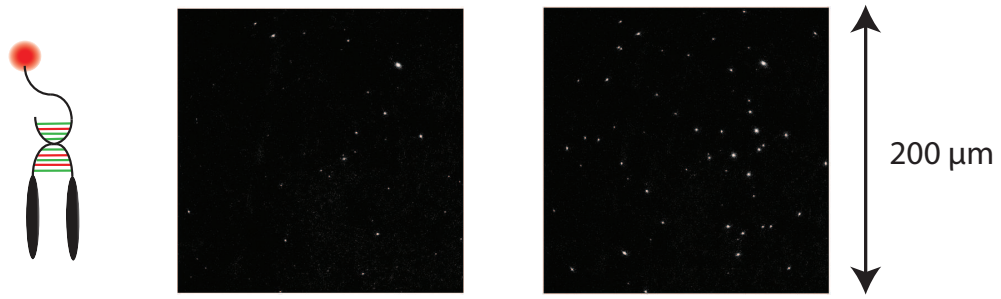

Figure 6.4: *Single vesicles attaching are easily distinguished and the label-transfer is small during the time-period for this study. The width of one frame is* $\approx 200\,\mu m$*. The time between the frames is about 1 hour.*

Using ds-2TAM/3 for labeling of vesicles containing the CXCR3 receptor seems to be the best of the three alternatives evaluated here. Single vesicles are distinguishable and the label-transfer is small. However, in this study, the concentration of vesicles is fairly low, which contributes to the moderate label transfer. Increasing the concentration leads to a more pronounced label transfer reducing the signal-to-noise ratio. This makes it more difficult to track many bind and release events for a longer time, to obtain better statistics. A disadvantageous

trade-off is thus present between the number of binding-events that can be studied and the time for the study.

Being able to detect single vesicles attaching to the surface with the fluorescent ds-2TAM/3 in the vesicle membrane leads to the next step in the project. The CXCL10 will be immobilized on the surface and ds-2TAM/3-labeled vesicles containing the CXCR3 receptor will be added. This will be done in a microtiter well and the number of attached vesicles and their residence times will be monitored in a so called equilibrium fluctuation study with TIRFM.

"An experiment is a question which science poses to Nature and a measurement is the recording of Nature's answer."

Max Planck

7

Equilibrium fluctuation analysis

Successful immobilization of ligands on the surface and fluorescent labeling of the receptor-containing vesicles leads to the actual measurements of the kinetic parameters describing the ligand-receptor interaction between the CXCL10 molecule and the CXCR3 receptor. How the different kinetic parameters can be determined and their actual interpretation has already been slightly touched upon in chapter 3. The conventional method for measuring these parameters includes both injection and rinsing. Furthermore, several different concentrations of ligands must be used to determine the equilibrium dissociation constant, K_d, explicitly. Figure 3.2 and 3.3 concludes this well.

Now, another method for determining the kinetic parameters will be undertaken, called equilibrium fluctuation analysis [3], with single molecule resolution [27, 28]. As the name of the method reveals the measurements are done under equilibrium conditions, which implies that multiple injection and rinsing steps are eliminated. However, kinetic parameters can be extracted describing *in vivo* processes occurring under non-equilibrium conditions [3]. By looking at many single binding events on a surface, in this case in a microtiter well with TIRF, statistics are obtained from which k_{on} and k_{off} can be extracted. By then adding a competitive ligand, an antagonist, to the bulk, the effective concentration of receptors can be lowered, via inhibition described in section 3.3. In this way the equilibrium dissociation constant, K_d, can be determined explicitly as well. Figure 7.1 illustrates the essential constituents of an equilibrium fluctuation analysis.

With the TIRF microscope it is possible to follow the actions on the substrate surface. Monocromatic light is totally reflected at the interface between substrate and liquid creating an evanescent field in which fluorophores on the surface can be excited. The emitted photons are then captured by a CCD camera and an image is created. To avoid photo-bleaching when the surface is studied for longer times snapshots are taken every 20 seconds with an exposure time of about 200 ms. The surface is photographed in this way for about an hour resulting in more than 100 pictures. The picture stack is then exported to Matlab for further image analysis. The time between frames as well as the total time is adjustable and is set according to how fast the kinetics are for the specific interaction studied.

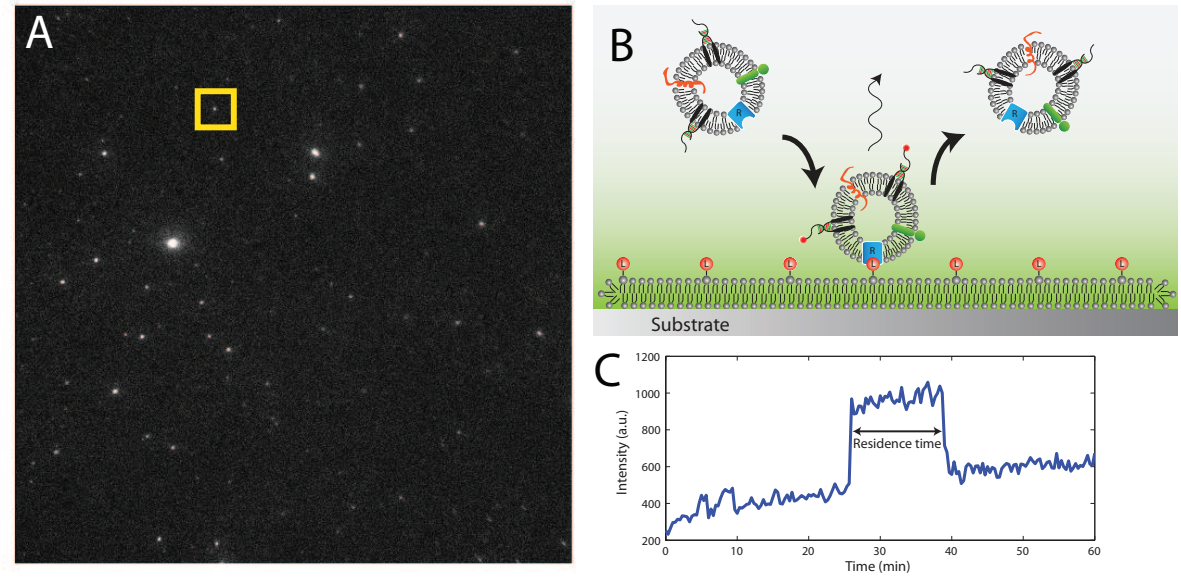

Figure 7.1: ***(A)*** *A typical snapshot from the TIRF microscope while doing equilibrium fluctuation measurements. The bright spots are labeled vesicles attached to the surface.* ***(B)*** *A schematic illustration of an interaction between ligand (L) and receptor (R). The vesicle holding the receptor first attaches to the surface, where it gets visible due to the emission of excited fluorophores incorporated into the vesicle membrane. After a while the vesicle detaches from the surface and it is no longer visible.* ***(C)*** *Average intensity plotted as a function of time of an area indicated with a square (yellow) in (A). Compare this plot with the schematic illustration above. The residence time is indicated with the double arrow. Note the increasing average intensity of the background, which is due to label transfer.*

7.1 Image analysis

The bright spots appearing on the surface in the field of view of the microscope are either receptors binding to the ligands, so called specific binding, or vesicles containing the receptor binding to something else on the surface, termed unspecific binding. Image analysis is performed to separate specific interactions from all interactions registered. A Matlab program written by Peter Jönsson in 2007 was used for this matter. The picture stack is imported and each pixel in the frames is assigned an intensity value according to its brightness. Three different thresholds are set by the user to define what counts as a binding event, how much the brightness of a vesicle can fade before it is considered bleached and what counts as a release-event.

It is only possible to extract a residence time of a binding event if the receptor binds and unbinds during the time-frame of the experiment. Vesicles must stay bound for at least three consecutive frames, which corresponds to about one minute in this experiment, in order to count as bind and release events. Vesicles never released are considered irreversibly bound, while those only visible in one or two frames as only diffusing in the evanescent field near the surface. Specific interactions are discriminated from unspecific by comparison between the positive control and the negative control, where no ligands are present on the surface. Both faster and slower interactions can be studied with the same technique by changing the setting of the camera connected to the microscope.

7.2 Determination of kinetic parameters

By sorting out the specific interactions and find their residence times, k_{off} can be extracted from a constructed plot with the number specifically bound vesicles remaining on the surface as a function of time. The plot is analogous to the rinsing part of figure 3.2. The number of vesicles attached to the surface after rinsing as a function of time is theoretically expressed as

$$\Theta(t) = \frac{\Theta_{max} k_{on} C}{k_{on} C + k_{off}} \exp\left(-k_{off} t\right) = A \exp\left(-k_{off} t\right) \tag{7.1}$$

which justifies an exponential fit to determine k_{off}.

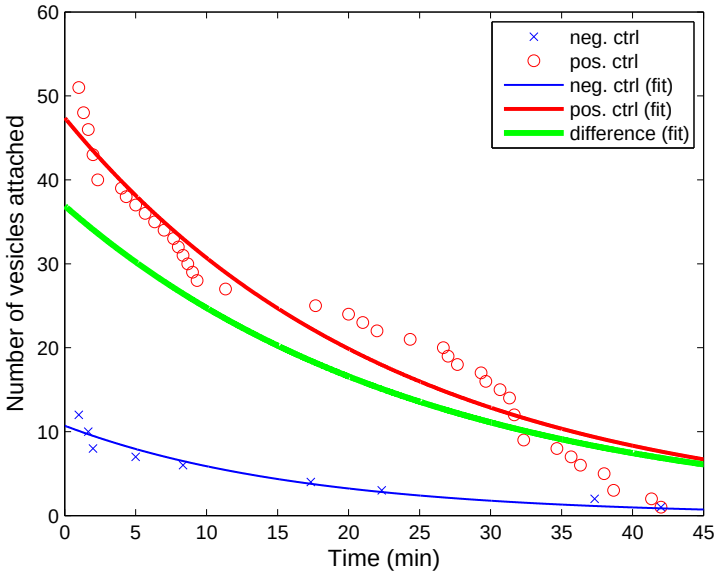

Figure 7.2: *Number of vesicles attached to the surface as a function of time. The curves are generated from the residence times of the binding events. Fewer bind and release events are seen in the negative control, which is predicted from previous QCMD experiments. The negative control is subtracted from the positive to determine k_{off} for the interaction.*

Both the positive and negative controls were fitted with single exponential functions. By subtracting the negative control from the positive the specific events are sorted out. k_{off} is then determined by fitting a single exponential function to this difference, according to equation (7.1).

The calculated k_{off} is $6.7 \cdot 10^{-4}\ s^{-1}$, which corresponds to a characteristic residence time of around $1500\ s$.

To determine k_{on}, the total number of vesicles adsorbed to the surface, Θ_+, is considered. By looking at the cumulative vesicle attachment the negative term in equation (3.3) vanishes, which yields

$$\frac{d\Theta_+(t)}{dt} = k_{on}C\left(\Theta_{max} - \Theta(t)\right) \tag{7.2}$$

with the approximation that $\Theta_{max} \gg \Theta(t)$, i.e. that the total number of ligands is much greater than the number of ligands with a receptor bound to it, the expression simplifies to

$$\frac{d\Theta_+(t)}{dt} = k_{on}C\Theta_{max} \tag{7.3}$$

where Θ_{max} is the total number of ligands, which is very difficult to quantify experimentally because of the extremely low surface coverage. In this project, Θ_{max} is estimated from the number of maleimide groups on the surface ($1/\mu m^2$) and the assumption that all of them have a bound CXCL10 molecule.

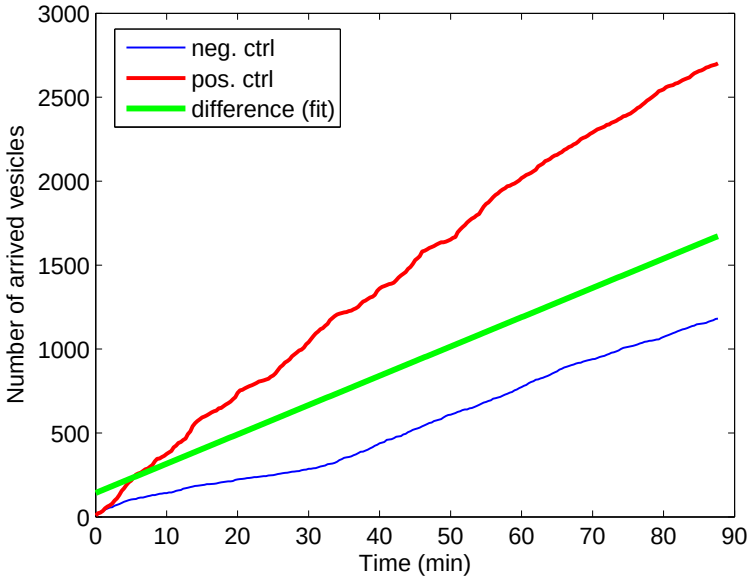

Figure 7.3: *Total number of arrived vesicles as a function of time. The negative control is subtracted from the positive and a linear fit is done to determine k_{on}.*

To sort out the specific binding events the negative control is subtracted from the positive. The difference is fitted to a linear function and k_{on} is calculated from equation (7.3). $d\Theta_+(t)/dt$ is the slope of the fitted line, the receptor concentration is 49 pM and Θ_{max} is about $1.5 \cdot 10^5$.

The calculated value of k_{on} is $4.0 \cdot 10^5\ s^{-1}M^{-1}$. The ratio between the explicitly calculated values of k_{off} and k_{on} is the implicitly determined equilibrium dissociation constant K_d. It is calculated to 16.8 nM, which can be compared to the reference literature value of 12.5 nM [6].

"Everything should be made as simple as possible, but not one bit simpler."

Albert Einstein

8

Theoretical aspects

A THEORETICAL FRAMEWORK of a complex system being studied is often valuable in the context of gaining further understanding of the system. Comparing results from experiments with theoretical calculations gives useful insights about the system and facilitates further research. In order to make rough estimates of the behaviour of a system or the outcome of an experiment the use of simplified models is invaluable. It both saves time and may give you a hint on whether the different outcomes of the experiment are feasible or not.

In this chapter a theoretical framework for the interaction between ligands and receptors is presented. A simple lattice model is adopted, that holds for both 1,2 and 3 dimensions. To stick to the common nomenclature we will first consider many ligands together with only one receptor. However, in this project the ligands are immobilized and receptors are diffusing above. The interchanging between the two will be considered after the model is fully described.

As the lattice model name reveals the space is divided into discrete positions where the ingoing elements can be situated. Therefore, a finite number of different configurations appear, each one associated with a certain total energy. Theory from the thermodynamics is then used to analyze the simplified system in terms of probabilities. Furthermore, possible altering of the kinetic parameters by introducing a flow is studied.

8.1 Theoretical equilibrium dissociation constant

The model adopted from [9] is as already stated a lattice model and a 2D-representation is illustrated in figure 8.1. Small circular shapes (L) are ligands and the bigger shapes (R) are the receptors. The space is divided into discrete positions where the ligands and receptors can be located. The movement of the ligands is restricted to the different squares while the receptor is fixed. One may arrange the ligands in many different ways, but still there are only two different classes of arrangements. The first one, seen in figure 8.1a, is when no ligand has

bound the receptor. The second one, seen in figure 8.1b, is when the receptor has one ligand bound to it.

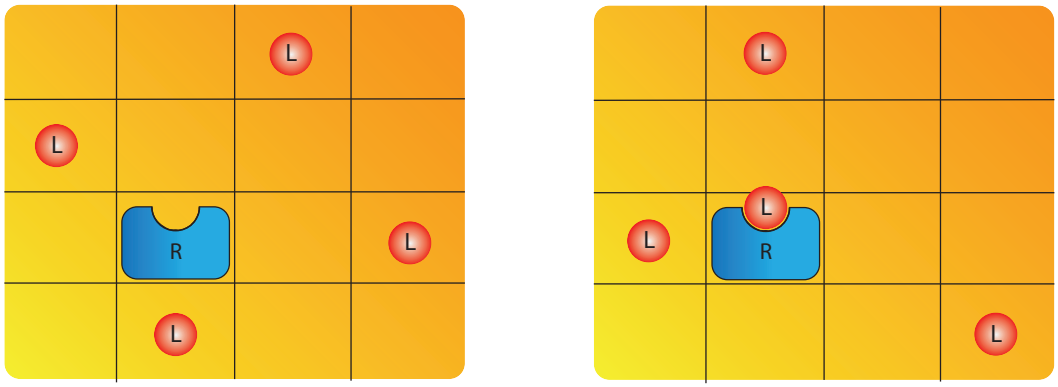

(a) **(b)**

Figure 8.1: *Two different types of arrangements of ligands are shown.* ***(a)*** *illustrates an arrangement where no ligand is bound to the receptor.* ***(b)*** *illustrates an arrangement where the receptor is occupied by a ligand.*

An expression for the probability of having the receptor occupied by a ligand will be derived in order to theoretically determine the equilibrium dissociation constant, K_d, which is interpreted as the ligand concentration at which the probability of having the receptor occupied equals 0.5. This can be compared to the Langmuir theory, treated in section 3.2, where K_d was interpreted as the receptor concentration when the equilibrium coverage was 0.5.

The expression for the probability is derived as a ratio between Boltzmann factors, consisting of the multiplicity of the type of state and the energy associated with it. As seen in figure 8.1, there are only two different types of arrangements. Furthermore, having L ligands and Ω pockets for ligands to reside in, the number of possible arrangements can be written as

$$M_{unbound} = \binom{\Omega}{L} = \frac{\Omega!}{L!(\Omega - L)!} \approx \frac{\Omega^L}{L!} \tag{8.1}$$

where the last approximation is justified if $L \ll \Omega$. Similarly, for the bound states the multiplicity is

$$M_{bound} = \binom{\Omega}{L-1} = \frac{\Omega!}{(L-1)!(\Omega - (L-1))!} \approx \frac{\Omega^{L-1}}{(L-1)!} \tag{8.2}$$

The energy associated with an unbound ligand is $\epsilon_{unbound}$ and for a bound ligand ϵ_{bound}. Thus, the energy associated with a certain arrangement, a so called microstate, where the receptor is unoccupied is $L\epsilon_{unbound}$ and for a microstate with an occupied receptor the energy is $(L-1)\epsilon_{unbound} + \epsilon_{bound}$. The probability of having a ligand bound to the receptor is then written as the sum of the Boltzmann factors for the bound microstates divided by the sum of the Boltzmann factors for all microstates.

$$P_{bound} = \frac{\frac{\Omega^{L-1}}{(L-1)!}e^{-\beta[(L-1)\epsilon_{unbound}+\epsilon_{bound}]}}{\frac{\Omega^L}{L!}e^{-\beta L\epsilon_{unbound}} + \frac{\Omega^{L-1}}{(L-1)!}e^{-\beta[(L-1)\epsilon_{unbound}+\epsilon_{bound}]}} \tag{8.3}$$

where P_{bound} is the probability of having a ligand bound to the receptor and $\beta \equiv 1/k_BT$. By multiplying both the numerator and denominator by $(L!/\Omega^L)e^{\beta L\epsilon_{unbound}}$ the expression simplifies to

$$P_{bound} = \frac{(\frac{L}{\Omega})e^{-\beta\Delta\epsilon}}{1+(\frac{L}{\Omega})e^{-\beta\Delta\epsilon}} = \frac{(\frac{c}{c_0})e^{-\beta\Delta\epsilon}}{1+(\frac{c}{c_0})e^{-\beta\Delta\epsilon}} \tag{8.4}$$

where c is the ligand concentration, c_0 is the highest possible concentration of ligands and $\Delta\epsilon = \epsilon_{bound} - \epsilon_{unbound}$. c_0 is derived from the size of the pockets that the ligands can reside in. The ratio between occupied and available pockets can also be interpreted as a ratio between volumes: occupied volume divided by total volume. This removes the simplification of the model that location and movement of ingoing elements are restricted to certain positions.

Until now, the receptors have been immobilized. In this project the setup has been somewhat turned around. The receptors are diffusing above the immobilized ligands. Therefore, from now, all concentrations instead refer to the receptors and the vesicles containing them.

The way to find the K_d is to find c when P_{bound} in equation (8.4) equals 0.5. $\Delta\epsilon$ is interpreted as the change in binding energy when forming the ligand receptor complex. P_{bound} has been plotted as a function of ligand concentration for three different chemokine ligands of CXCR3, namely CXCL9, CXCL10 and CXCL11, see figure 8.2a. The energy gain associated with each of the complexes is stated in table 8.1. The values are from [26], where the structures of the ligands and receptor have been modeled by first extracting the amino-sequence of the proteins and then compared with proteins in databases.

Table 8.1: *Change in energy associated with binding for three different CXCR3-complexes. The energy is given in four different units.*

Ligand-Receptor complex	kcal/mol	eV	k_BT	J
CXCL9/CXCR3	-3.8	-0.16	-6.3	$-2.6 \cdot 10^{-20}$
CXCL10/CXCR3	-4.1	-0.18	-6.8	$-2.8 \cdot 10^{-20}$
CXCL11/CXCR3	-6.9	-0.30	-11.5	$-4.7 \cdot 10^{-20}$

By putting P_{bound} equal to 0.5 and c to K_d equation (8.4) can be rearranged to

$$K_d = c_0 e^{-\beta\Delta\epsilon} = c_0 e^{-\Delta\epsilon/k_BT} \tag{8.5}$$

It is evident that K_d is dependent of the energy gain associated with the ligand-receptor complex, but also the maximum concentration of vesicles containing a receptor. This in turn is related to the size of the vesicles. However, it should be pointed out already at this point that the rotational degree of freedom, which is omitted in this model, will balance the influence

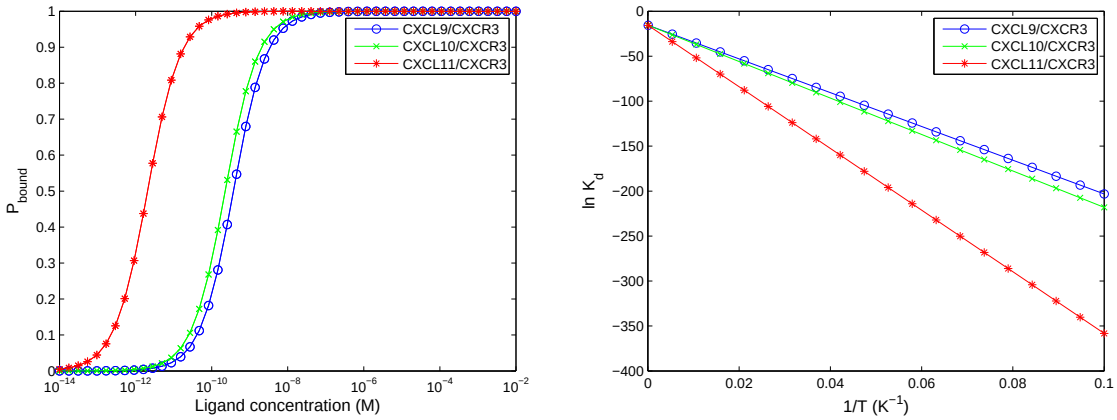

Figure 8.2: ***(a)*** *The probability of having a vesicle, of diameter* 250 *nm, containing a receptor attached to an immobilized ligand as a function of receptor concentration for three different ligand-receptor complexes.* ***(b)*** *van't Hoff plot for the three different chemokine ligands with a vesicle size of* 250 *nm.*

of vesicle size on K_d to some extent. For a larger vesicle the relative number of rotational positions enabling association with a ligand is lower than for smaller vesicles. Thus, there are more configurations on average for larger vesicles with receptors that do not result in binding, yielding a higher K_d.

The equilibrium dissociation constant, K_d, is theoretically calculated from expression 8.5 for the three different ligand-receptor complexes with two different vesicle sizes. The result is seen in table 8.2.

Table 8.2: *Theoretical equilibrium dissociation constant, K_d, for three different ligand-receptor complexes for receptor-carrying vesicle sizes of* 100 *nm and* 250 *nm.*

Ligand-Receptor complex	100 nm	250 nm
CXCL9/CXCR3	7.5 nM	0.45 nM
CXCL10/CXCR3	4.3 nM	0.26 nM
CXCL11/CXCR3	0.027 nM	0.0016 nM

The ligand used in this project is the CXCL10 and the average size of the receptor-containing vesicles is 250 nm. This gives a K_d of $\approx 0.3\,nM$, which can be compared to the implicitly determined value of 16.8 nM. However, it should be noted that this model only considers pure translation of receptor-containing vesicles. Adding rotation of the vesicles as another degree of freedom will make the number of possible configurations larger resulting in a larger theoretical K_d.

8.2 Changes in enthalpy and entropy

Equation (8.5) has the same fundamental form as the Arrhenius equation [29]

$$k = k_0 e^{-E_a/k_B T} \tag{8.6}$$

which describes the rate of chemical reactions. k_0 is a constant interpreted as the rate corresponding to an activation energy, E_a, of zero. By taking the logarithm of both sides of equation (8.5) the result is

$$ln(K_d) = -\frac{\Delta\epsilon}{k_B}\frac{1}{T} + ln(c_0) \tag{8.7}$$

where both K_d and c_0 is normalized to a concentration of $1\,M$. The change in standard Gibbs free energy is related to the equilibrium constant of a chemical process, K, by

$$\Delta G^0 = -RTln(K) \tag{8.8}$$

where R is the gas constant and T is the temperature and K is normalized to $1\,M$. By describing Gibbs free energy in terms of enthalpy and entropy the expression can be rewritten as

$$ln(K) = -\frac{\Delta H^0}{R}\frac{1}{T} + \frac{\Delta S^0}{R} \tag{8.9}$$

where ΔH^0 is the standard enthalpy change and ΔS^0 is the standard entropy change. Here K is normalized and is thus without unit. The expression can be compared to equation (8.7). The analogous to a van't Hoff plot is seen figure 8.2b. The expression for $ln(K_d)$ in equation (8.7) has been plotted against the inverse temperature, $1/T$. Equation (8.7) and (8.9) have the same fundamental appearance. ΔH^0 can be derived directly from $\Delta\epsilon$. Similarly ΔS^0 is related to $ln(c_0)$. See table 8.3 for the results.

Table 8.3: *Change in standard enthalpy and standard entropy upon association between the CXCR3 receptor and the CXCL10 ligand. Two different vesicle sizes are presented.*

Ligand-Receptor complex	$\Delta H^0\,[J]$	$\Delta S^0\,[J/(mol \cdot K)]$
CXCL10/CXCR3 ($100\,nm$)	$-0.28 \cdot 10^{-19}$	-105.3
CXCL10/CXCR3 ($250\,nm$)	$-0.28 \cdot 10^{-19}$	-128.1

According to these results of the lattice model the change in standard enthalpy upon association is not dependent of the size of the vesicle carrying the receptor. However, the change in standard entropy is dependent on the size of the vesicle.

8.3 Influence of flow

A possible future development of the used method to study ligand-receptor interactions on a single molecule level would be to use a microfluidic channel instead of a microtiter well. The advantage of the microfluidic channel is that the material consumption is very small and that

a flow can be introduced. The idea is to be able to alter equilibrium coverage and kinetic rates in an easier way. In this section calculations are made in order to estimate whether a flow in a microfluidic channel may affect the interaction between a ligand and a receptor-containing vesicle.

Theoretical calculations often involves simplifications and estimates. To evaluate whether a flow may affect the interaction a useful approach is to exaggerate critical parameters involved. The idea is to overestimate the effect of the flow and in that way be able to reject the effect if it is small enough.

The cross sectional dimensions of a microfluidic channel is set to $150x150\mu m$ and the maximum flow rate to 300 $\mu l/min$. The vesicle diameter is set to 250 nm. With bilayer and molecules for connection the center of the vesicle is about 130 nm above the channel floor.

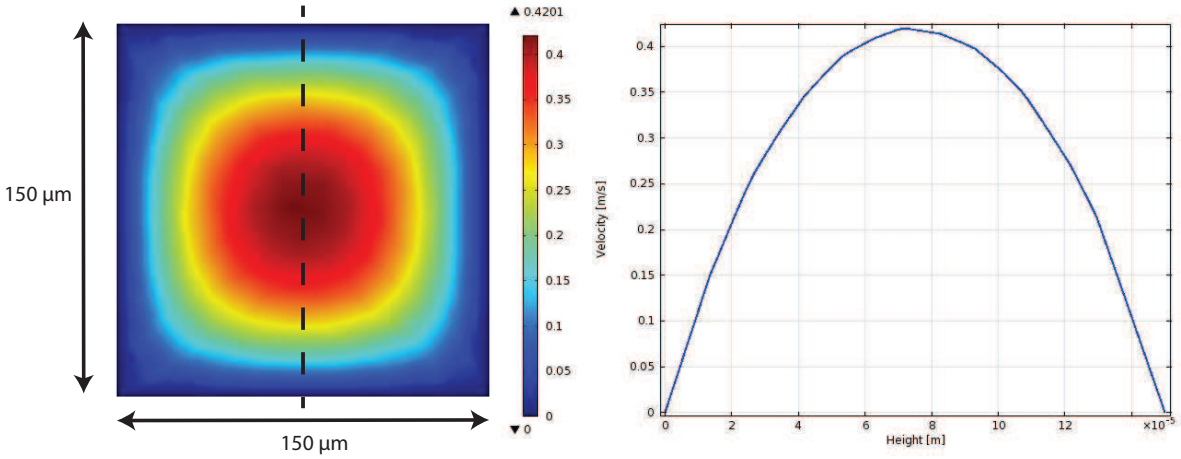

Figure 8.3: *A microfluidic channel with cross sectional dimensions* $150x150\ \mu m$ *was simulated in Comsol Multiphysics.* ***(a)*** *Velocity profile in a cross section of the channel. The bar to the right translates color to velocity. The flow velocity unit is [m/s].* ***(b)*** *The velocity plotted along the dashed line in the left figure. Unit on x-axis is [m] and on the y-axis [m/s].*

From the simulation of a microfluidic channel, see figure 8.3, a maximum flow velocity affecting the vesicles attached to the surface can be extracted. Since the dimension of a vesicle is so small the flow affecting it increases almost linearly with height. Thus, the average flow corresponds to the flow at the center-height of the vesicle set to $130nm$, which is approximately $1.5mm/s$. To calculate the force exerted on the vesicle when the flow is maximized the Stoke's drag expression [9] is used

$$F_s = 6\pi\eta Rv = 6\pi \cdot 10^{-3} \cdot 125 \cdot 10^{-9} \cdot 1.5 \cdot 10^{-3} \approx 3.5\, pN \tag{8.10}$$

where η is the viscosity of the surrounding medium, in this case water, R is the radius of the vesicle and v is the flow velocity.

When studying ligand-receptor kinetics it is sometimes useful to separate bond formation/rupture in two different phases, as shown in equation (3.1). It was suggested by George Bell that the

rate of bond dissociation was dependent on an applied force [17]. The relationship he suggested was

$$r_-(F) = r_-(0)e^{\gamma F/k_B T} \tag{8.11}$$

where r_- is the rate of bond rupture, F is the applied force and γ is a parameter that should be close to the interaction range of ligand-receptor bonds. Bell suggested that the value of γ should be around $0.5\,nm$.

By inserting the estimated maximum force of $3.5\,pN$ into equation (8.11) a new bond rupture rate is obtained which is higher than that for a ligand-receptor complex not affected by an external force.

$$r_-(F) = r_-(0)e^{\gamma F/k_B T} = [F = 3.5\,pN, \gamma = 0.5\,nm] \approx r_-(0) \cdot 1.5 \tag{8.12}$$

This result suggests that a substantial flow may alter the kinetics of ligand-receptor interactions. However, without the large vesicles holding the membrane receptors the force would be just a fraction of the calculated, thus reducing the effect of the flow on the bond rupturing rate drastically.

Tweaking kinetic parameters describing ligand-receptor interactions by performing measurements in a microfluidic channel is a very difficult task. Since the flow is not uniform where the ligands are immobilized a larger force will be exerted on some of the vesicles. The broad size distribution of vesicles containing the receptors also makes it more difficult to control the force exerted on the vesicles.

"I am prepared to go anywhere, provided it be forward."

David Livingstone

9

Conclusions

Experimental work often includes many different steps leading to the actual measurements or observations. Every single step in the process is a source of error, often difficult to quantify and keep track of, making laboratory work different from other types of scientific professions. A lot of trial and error lies behind many of the famous experimental breakthroughs, which is often forgotten, but very fascinating indeed.

In this project a platform for studying the kinetics of the interaction between the human chemokine CXCL10 and its transmembrane receptor CXCR3 has been evaluated. The results from the different experimental steps leading to the characterization of this interaction will be summarized in this section along with theoretical results on the actual setup and future perspectives.

The major finding is that it is possible to use equilibrium fluctuation analysis to characterize the kinetics of a chemokine-GPCR interaction. The fundamental setup is possible to apply on natural ligand-receptor systems in order to evaluate new drug candidates, which is very interesting for drug development industry. Being able to identify promising drugs in a cost-effective and time-saving way could revolutionize the whole drug discovery process.

9.1 Immobilizing ligands on a surface

Having a bilayer as a foundation for the immobilized ligands seems to work well according to the QCMD-plot in figure 5.2. There is a clear distinction between the positive and negative control suggesting that a considerable fraction of the receptors bind specifically to the immobilized ligands. However, it should be pointed out that unspecific binding occurs, but is not so pronounced in the plot because of the limited sensitivity of the instrument. Unspecific binding is visible in the TIRF setup with the same chemistry in the microtiter wells, which is due to the higher sensitivity.

9.2 Fluorescent labeling of cell mimics

Three different cell dyes were tested for labeling of the vesicles containing the membrane receptor. The requirements were that the dye would incorporate into the vesicle membrane and make separate vesicles visible in the TIRF microscope. Furthermore, the transfer of dye to the surface where the ligands were immobilized would be very low. The dye that met these requirements the best was the ds-2TAM/3, the cholesterol-DNA with rhodamine. However, a small label-transfer was observed which complicated longer measurements as well as having higher concentrations of vesicles in bulk.

9.3 Equilibrium fluctuation analysis

Studies on the kinetics of the interaction between the CXCL10 ligand and the CXCR3 receptor was done using a bilayer as a foundation. Separate bind/release events were observed using the ds-2TAM/3 for labeling of the vesicles. However, the number of such events was fairly small making the determination of the kinetic parameters rather difficult. To get better statistics more events need to be observed. Increasing the concentration of vesicles would increase the number of events, but at the same more ds-2TAM/3 would incorporate into the bilayer complicating the image analysis. Studying the surface for a longer time would lead to the same problem. However, it is evident that this fundamental setup can be used to extract kinetic information from the interaction. For the CXCL10/CXCR3-interaction k_{off} was determined to $6.7 \cdot 10^{-4}\, s^{-1}$ and k_{on} to $4.0 \cdot 10^{4}\, s^{-1} M^{-1}$. The implicit K_d, defined as the ratio between the explicit k_{off} and k_{on}, was calculated to $16.8\, nM$. This can be compared to the reference literature value of $12.5\, nM$ [6].

9.4 Theoretical aspects

A simple lattice model was introduced to determine the equilibrium dissociation constant, K_d, theoretically. For the CXCL10/CXCR3 interaction K_d was calculated to $0.3\, nM$, which in comparison to the experimental value is about a factor 50 smaller. However, by introducing rotation of receptor-containing vesicles to the model the estimated K_d would increase. The theoretical background is a very useful tool that can be used to give a foundation to corresponding experiments. Comparing experimental results with theoretical calculations may strengthen the validity of the study performed. Change in standard enthalpy and standard entropy describing the ligand-receptor interaction could also be extracted from the lattice model.

Introducing a flow to a setup similar to the one used in this project but with a microfluidic channel instead of a microtiter well may affect the kinetics of the interaction studied. If the liquid flow at the ligand-receptor complex is at a practical maximum the parameter k_{off} can be increased several tens of percent. However, it should be stated that it is very difficult to keep track of the effect of the flow since vesicles are affected differently depending on their position in the microfluidic channel as well as their size.

"I got an idea, an idea so smart my head would explode if I even began to know what I was talking about."

Peter Griffin

10

Future perspectives

The work conducted in this master thesis project has lead to many important insights in studying the kinetics of the interaction between a ligand and membrane receptor on a single molecule level. The different steps leading to the goal of determining kinetic parameters for an interaction between a GPCR and one of its ligands have involved immobilization of ligands on a surface, fluorescent labeling of membrane derived vesicles and equilibrium fluctuation analysis.

The fundamental setup used in this project seems promising, but there are some problems remaining to be solved in order to fully characterize the kinetics of the interaction between CXCL10 and CXCR3. For example the label-transfer needs to be reduced in order to be able to increase the amount of vesicles attaching to the surface and increase the measuring time. This in order to get more statistics and be able to clearly distinguish specific binding from unspecific. For this, the way of labeling membrane derived vesicles can be further investigated. Another approach would be to go for another foundation different from a lipid bilayer. An alternative would be to use a gold surface and couple the ligands via a thiol-PEG chemistry. Emitted light from fluorescent molecules transferred to the surface will then be quenched by the gold [30], which may reduce the background signal drastically, see figure 10.1.

The method investigated in this thesis opens up for further developments in order to characterize the interaction between ligand and receptor, both in bulk, see figure 10.1. By adding ligands in the bulk and study the changes in the kinetics of the interactions occurring on the surface information about the interaction between ligand and receptor in bulk may be obtained. This interaction better represents that occurring in the body since neither the ligand or the receptor is immobilized.

Going even further into the future it is likely that a technique based on single molecule detection is used to characterize potential drugs. This project is only one small step towards the future techniques used for drug discovery.

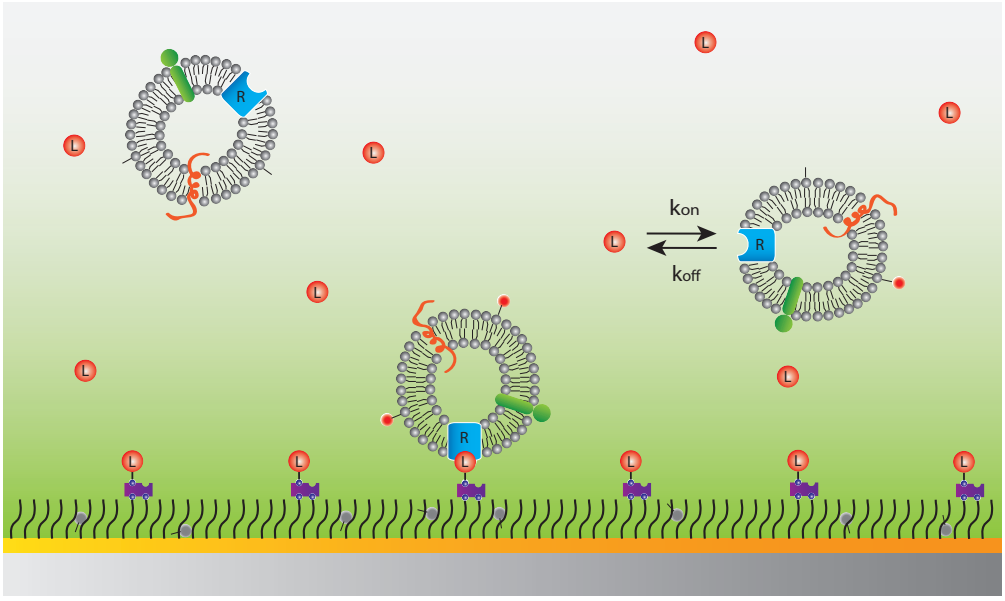

Figure 10.1: *By immobilizing ligands on a thin sheet of gold with a thiol-PEG chemistry fluorescent molecules transferred to the surface will be quenched by the gold, which reduces the background signal. By adding ligands (L) in the solution that binds to the receptors the number of detected ligand-receptor interactions per time unit is reduced. This information can be used to calculate the kinetic parameters for the interaction occurring in bulk, which better represents what happens inside the body.*

Bibliography

[1] R. Evans, A. Noyau, *The atomic nucleus*, McGraw-Hill New York, 1955.

[2] D. Holmes, A. Caldwell, Give me a lever and a place to stand and I'll move the world, *Physics Education* **47** (2012) 264–265.

[3] A. Gunnarsson, et al., Kinetics of Ligand binding to Membrane-Receptors from Equilibrium Fluctuation Analysis of Single Binding Events, *J. Am. Chem. Soc.* **133** (2011) 14852–14855.

[4] N. Robertson, et al., The properties of thermostabilised G protein-coupled receptors (StaRs) and their use in drug discovery, *Neuropharmacology* **60** (2011) 36–44.

[5] S. Moro, G. Spalluto, K. Jacobson, Techniques: Recent developments in computer-aided engineering of GPCR ligands using the human adenosine A_3 receptor as an example, *Trends Pharmacol. Sci.* **26** (2005) 44–51.

[6] C. Heise, et al., Pharmacological characterization of CXC chemokine receptor 3 ligands and a small molecule antagonist, *J. Pharmacol. Exp. Ther.* **313** (2005) 1263–1271.

[7] P. Davies, *The fifth miracle: The search for the origin and meaning of life*, Touchstone Books, 2000.

[8] D. Wacey, et al., Microfossils of sulphur-metabolizing cells in 3.4-billion-year-old rocks of Western Australia, *Nature Geosci.* **4** (2011) 698–702.

[9] R. Phillips, J. Kondev, J. Theriot, *Physical biology of the cell*, Garland Science New York, 2009.

[10] R. Breslow, Hydrophobic effects on simple organic reactions in water, *Accounts Chem. Res.* **24** (1991) 159–164.

[11] R. Jones, *Soft Condensed Matter*, Oxford University Press, 2002.

[12] S. Singer, G. Nicolson, The fluid mosaic model of the structure of cell membranes, *Landmark Papers in Cell Biology* (1972) 296–307.

[13] M. Karnovsky, et al., The concept of lipid domains in membranes., *J. Cell Biol.* **94** (1982) 1–6.

[14] A. Granéli, et al., Formation of supported lipid bilayer membranes on SiO_2 from proteoliposomes containing transmembrane proteins, *Langmuir* **19** (2003) 842–850.

[15] S. Scheindlin, A brief history of pharmacology, *Modern Drug Discovery* **4** (2001) 87–88.

[16] H. Rang, et al., *Rang and Dale's Pharmacology*, 6th Edition, Edinburgh: Churchill Livingstone, 2007.

[17] P. Bongrand, Ligand-receptor interactions, *Rep. Prog. Phys.* **62** (1999) 921–968.

[18] D. Myszka, R. Rich, Implementing surface plasmon resonance biosensors in drug discovery, *Pharm. Sci. Technol. To.* **3** (2000) 310–317.

[19] T. Blundell, H. Jhoti, C. Abell, High-throughput crystallography for lead discovery in drug design, *Nature Reviews Drug Discovery* **1** (2002) 45–54.

[20] I. Hemmilä, S. Webb, Time-resolved fluorometry: an overview of the labels and core technologies for drug screening applications, *Drug Discov. Today* **2** (1997) 373–381.

[21] M. Cooper, Advances in membrane receptor screening and analysis, *J. Mol. Recognit.* **17** (2004) 286–315.

[22] R. Hummel, *Electronic Properties of Materials*, 3rd Edition, Springer Science, 2000.

[23] Q-Sense, `http://www.q-sense.com/qcm-d-technology`, accessed: 2012-01-31.

[24] Visit at Q-sense with Jennie Wikström, 2012-03-05.

[25] D. Axelrod, Cell-substrate contacts illuminated by total internal reflection fluorescence., *J. Cell Biol.* **89** (1981) 141–145.

[26] T. Trotta, S. Costantini, G. Colonna, Modelling of the membrane receptor CXCR3 and its complexes with CXCL9, CXCL10 and CXCL11 chemokines: Putative target for new drug design, *Mol. Immunol.* **47** (2009) 332–339.

[27] A. Gunnarsson, et al., Single-molecule detection and mismatch discrimination of unlabeled DNA targets, *Nano letters* **8** (2008) 183–188.

[28] A. Gunnarsson, et al., Kinetic and thermodynamic characterization of single-mismatch discrimination using single-molecule imaging, Nucleic Acids Res. **37** (2009) 1–8.

[29] K. Laidler, The development of the Arrhenius equation, *J. Chem. Educ.* **61** (1984) 494.

[30] E. Dulkeith, et al., Fluorescence Quenching of Dye Molecules near Gold Nanoparticles: Radiative and Nonradiative Effects, *Phys. Rev. Lett.* **89** (2002) 1–4.

A

List of abbreviations

- **DOPE** - 1,2-Dioleoyl-sn-Glycero-3-Phosphoethanolamine
- **GPCR** - G-Protein Coupled Receptor
- **NaAc** - sodium acetate
- **PBS** - Phosphate Buffered Saline
- **PEG** - poly(ethylene glycol)
- **POPC** - 1-palmitoyl-2-oleoyl-sn-glycero-3-phosphocholine
- **QCM-D** - Quartz Crystal Microbalance with Dissipation monitoring
- **SPR** - Surface Plasmon Resonance
- **TIRFM** - Total Internal Reflection Fluorescence Microscopy